Sizing Calculation of the ITER Compressed Air Supply for Tokamak Cooling Water Valve Actuators

ME55035: MSc Thesis

Marcell Szabo (6058299)

Delft University of Technology

TU Delft

Sizing Calculation of the ITER Compressed Air Supply for Tokamak Cooling Water Valve Actuators

by

Marcell Szabo (6058299)

Supervisor:	J.W.R. Peeters
Company Supervisor:	Nicolas Schiliuk
Faculty:	Faculty of Mechanical Engineering

Cover: ITER Tokamak and Plant Systems by ITER (Modified)

TU Delft

Preface

The present thesis explores the current state of design of the compressed air network for the ITER Tokamak Cooling Water System. The primary goal of the report is to verify the system's operability and identify relevant design gaps to accelerate future work.

I would like to express my gratitude to ITER for allowing me to pursue this opportunity, and Nicolas Schiliuk for his tireless efforts in providing me with every relevant material needed to execute this task at the highest level possible.

Marcell Szabo
Hajdúszoboszló, Hungary, October 2025

Abstract

This thesis presents the design and performance assessment of the Compressed Air System for Tokamak Cooling (26CATC) at ITER, which operates the Tokamak Cooling Water System (TCWS)—a critical component ensuring safe reactor cooling. The research addresses the challenge of ensuring reliable pneumatic valve operation within a highly constrained environment characterized by long piping networks, magnetic field limitations, and strict safety requirements. The main design gaps identified concern valve stroking times, excessive air consumption at several interface points, and the need for effective overpressure protection. To address these, a steady-state compressible flow model was developed using AFT Arrow, supported by detailed data extraction from 3D CAD geometries and automated processing tools to calculate flow resistances and mass flow rates for over a thousand valves. The methodology incorporated actuator and torque data to compute stroke times and evaluate compliance with safety and operational criteria. Results showed that while most valves meet the required performance, 21 safety-critical valves fail to achieve the necessary stroking times, requiring design modifications such as local pressure tanks or spring-assist systems. Additionally, more than 60% of consumption scenarios exceed predefined flow rate limits, highlighting the need for capacity optimization at several interface points. The network's overpressure protection was successfully addressed through the integration of 168 Pressure Reducing Valves, ensuring safe operation under all loading conditions. Overall, the study demonstrates that while the current design framework provides a robust foundation for the 26CATC system, targeted design improvements and further validation are required to guarantee full compliance and operational reliability in ITER's demanding environment.

Contents

1
Introduction

Some of today's most pressing issues related to energy include climate change [1], fossil fuel expansion in developing countries [2], energy independence [3], and economic viability of renewable energy production [4]. The global energy landscape remains highly imbalanced, with only a few countries controlling the majority of fuel resources [3]. This concentration of energy supply has fueled political debates, driven inflation, and, in some cases, provided leverage for violent activities [5]. Furthermore, the world's heavy reliance on fossil fuels makes their combustion the leading contributor to climate change [6]. The scarcity of accessible energy resources, combined with the growing challenges posed by climate change, underscores the urgent need for sustainable energy production in the future [7].

To address all points, nuclear fusion offers a promising solution. In a fusion reactor, light nuclei collide and fuse together under immense pressure and temperature within a plasma state, releasing energy. This reaction provides high-density, continuously available power without emitting harmful substances or greenhouse gases, and due to the extreme conditions necessary for fusion, it eliminates the additional risks of nuclear meltdowns or accidents associated with traditional fission reactors. The fuel used for fusion consists primarily of hydrogen isotopes, such as deuterium and tritium. Deuterium can be extracted from seawater, where it is abundant, while tritium can be bred within the reactor itself through reactions with lithium. Lithium is found in the Earth's crust and can also be sourced from seawater.[8]

Realizing the above, the first actions were taken at the Geneva Superpower Summit in November 1985, by General Secretary Gorbachev of the Soviet Union [9]. He presented the idea of a collaborative international project to US President Ronald Reagan, which ended in the foundation of ITER just a year later. Over the following years, engineers and scientists developed the plant's conceptual design, ultimately concluding in 2001 with the proposal of a final design that incorporated a tokamak reactor. The commissioning phase started in 2005 and is still ongoing 20 years later. Due to the tokamak's unique design, engineers are facing problems never encountered before and working on similarly unique solutions to overcome them. However, several systems are first-of-a-kind, which has resulted in significant issues with the reactor's core component: the vacuum vessel confining the burning plasma. This pushed the project's timeline out by a further 8 years, with the first plasma operation currently scheduled for 2033 [10]. Consequently, there are still a number of tasks missing and systems to be designed.

One such subsystem is the compressed air system for the pneumatically actuated valves inside the TCWS, which supplies the content of this thesis. The study starts by providing an overview on the physics background of nuclear fusion and the reactor's subsystems in Chapter 2. The Tokamak Cooling Water System (TCWS) is introduced in Chapter 3, detailing the actuated valves and the necessity of compressed air to operate them. The compressed air network itself is described in Chapter 4. The design goals of the thesis project are identified and collected in Chapter 5, while providing an overview of inherent uncertainties and network modelling. This marks the end of the literature study and introduction. The report then focuses on the developed method used to achieve the design goals in Chapter 6. The results are shown in Chapter 7. The study is concluded by listing the conclusions and the necessary future work to make the system fully operational in Chapter 8.

2

Background

Nuclear fusion occurs when two light atomic nuclei merge to form a heavier nucleus, releasing both mass and energy in the process. This reaction powers stars, making habitable conditions on Earth possible. However, fusion requires extreme temperatures to supply the energy needed to overcome electrostatic repulsion between positively charged nuclei. As a result, achieving controlled fusion in artificial settings remains a significant challenge.

There are several naturally occurring fusion reactions: the three most probable are deuterium-deuterium, deuterium-tritium and deuterium-helium. ITER has chosen to proceed with the deuterium-tritium reaction, which has the highest probability for particle collision, and requires the least temperature to get started [8].

The deuterium-tritium (D-T) reaction is shown in Eq. 2.1:

$$ {}_{1}^{2}H + {}_{1}^{3}H \rightarrow {}_{2}^{4}He + {}_{0}^{1}n + 17.6 \text{ MeV} \tag{2.1} $$

Eq. 2.1 highlights the energy yield and the participating nuclei, both making nuclear fusion an interesting candidate for energy production. In comparison to nuclear fission, the energy gained from the reaction is significantly lower than that of a single fission reaction (splitting ${}_{92}^{235}U$ yields around 200MeV). However, due to the lighter nuclei, the released energy per kg of fuel is approximately four times higher for fusion.

Secondly, the reaction uses deuterium (${}_{1}^{2}H$) and tritium (${}_{1}^{3}H$) as fuel. Both isotopes have abundant sources: deuterium is commonly found in our oceans, while tritium can be bred from the blanket system surrounding the fusion reaction by using Lithium. Again, Li is commonly available and can be further extracted from ocean water, covering the world's energy needs for ca. 6 million years [9].

Nevertheless, for the D-T reaction to occur, the fuel must be in a plasma state - a state where the temperature is so high that the electrons are separated from the nuclei, ionizing the matter. To contain the burning plasma, ITER made the design choice to use a tokamak, shown in Figure 2.1. A tokamak is a toroidal-shaped device that uses magnetic fields to contain and stabilize the hot plasma. Its closest component to the fusion reaction is the blanket module (1), which protects the superconducting magnets (3) from the thermal radiation and high-energy neutrons produced in the plasma, while breeding the necessary tritium for self-sustaining fusion. The magnets are used to heat, confine, stabilize, and control the plasma and are cryogenically cooled to reach superconductivity. Extracting the heat and ash from the fusion reaction, the divertor (2) acts as a ”magnetic drain” to the plasma, concentrating all the escaping heat and particles in a small area, resulting in heat fluxes more than four times higher than that experienced by a spacecraft entering Earth's atmosphere [11]. All the mentioned components are supported by the vacuum vessel (4), a double-walled steel container acting as the first safety containment boundary. The tokamak is further supported by the cryostat (5), which also provides a low-pressure vacuum environment to reduce heat transfer to the magnets. Although not explicitly shown on the figure, the blanket (1), the divertor (2) and the vacuum vessel (4) are all directly cooled by the Tokamak Cooling Water System, described in Chapter 3.

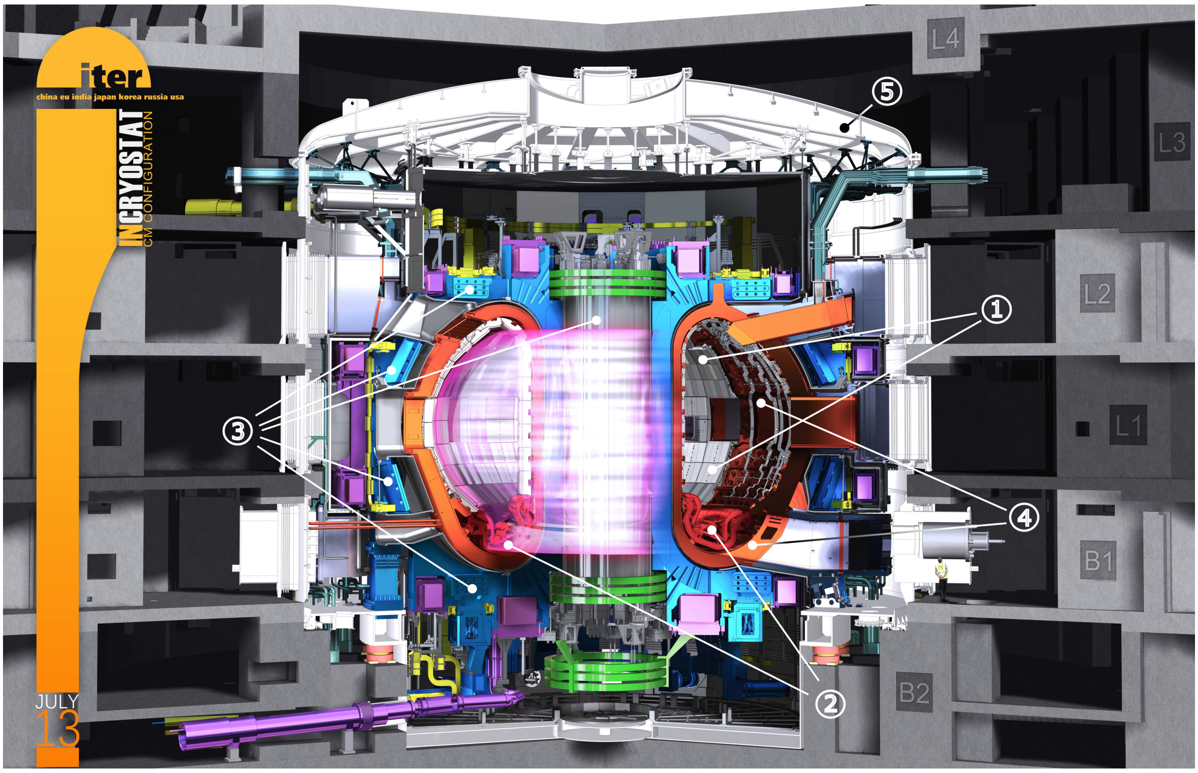

Figure 2.1: The most important components of ITER's reactor. (1) Blanket, (2) Divertor, (3) Magnets (4) Vacuum Vessel, (5) Cryostat. Source:[9]. Modified by Marcell Szabo, 2025.

The complexity of the necessary systems highlights yet another aspect for nuclear fusion: safety. Generally, nuclear safety is inherently better in fusion than fission power. At ITER, a runaway reaction or a nuclear accident such as the Fukushima one is impossible: a small perturbation in the fuelling process leads to an immediate cease of the reaction, and the residual heat is never enough to melt the surrounding blanket system's material. This means that even for a catastrophic break inside the Tokamak, irradiation to the surroundings will be very low [9]. As a consequence, cooling is not a safety function and confinement boundaries will not be affected even in the total loss of coolant. Thus, the primary safety objective for D-T fusion remains the confinement and handling of tritium and other activated corrosion products inside the vacuum vessel and the cooling water. High activity, long-lived radioactive waste is not produced by ITER, as the reaction exhaust is inert helium gas (see Eq. 2.1), and the activated materials are classified as very low, low, or medium activity waste. This makes fusion power not only a reliable and high-density energy source, but also significantly safer than traditional fission power plants.

Although nuclear fusion is a widely-researched topic, the technology making the operation of a fusion power plant possible is still lacking. ITER's goal is to bridge this gap and demonstrate that, with engineering innovation and international collaboration, nuclear fusion on a power-plant scale can be achieved. As a guidance, the ITER Research Plan [10] was created and touches on one of the key commercial factors unresolved: a self-sustaining fusion reaction. To define such, the fusion energy gain factor Q has been introduced, giving the ratio between the input power to heat the plasma and the output power of the reaction:

$$Q = \frac{P_{out}}{P_{in}} \tag{2.2}$$

By increasing the factor over unity, ITER aims to demonstrate a self-sustaining reaction, while $Q = 10$ would indicate commercial potential for future fusion power plants. To further establish feasibility and advance fusion research, the Plan sets a target of routine operation with 500 MW power and $Q \geq 10$ as an objective for burn durations of 5-8 minutes. Additionally, it aims for sustained operation lasting up to 1 hour in steady-state, non-inductive mode with $Q \geq 5$. These objectives are not solely physics milestones, but also define the main loading conditions for the Tokamak Cooling Water System (TCWS), which is the focus of this literature study.

Although ITER will itself not convert plasma heat into electricity, it paves the way for future commercial fusion power plants that will. The key component in such future reactors is their Cooling Water System (CWS), serving as the primary instrument conveying the heat between reactor components and the steam turbine. The challenges faced in the CWS - and particularly, the TCWS - due to fusion's exceptional nature are examined in detail in Chapter 3.

3

The Tokamak Cooling Water System

3.1. Introduction and system description

As an integral and crucial part of the ITER project, the Cooling Water System (CWS) provides cooling to almost all the project's different parts [12]. It regulates the thermal-hydraulic parameters of ITER's systems and transfers their heat loads to the environment during plasma operation and decay heat removal. The system's nominal heat load is 550 MW, with a peak load of approximately 1150 MW.

The CWS is divided into four separate systems:

- Tokamak Cooling Water System (TCWS): The primary closed-loop circuit designed to remove 1000 MW of power from three Primary Heat Transfer Systems (PHTSs): Vacuum Vessel (VV), Integrated Blanket, ELM[1] and Divertor (IBED), and the Neutral Beam Injectors (NBI[2]).
- Component Cooling Water System (CCWS): A secondary loop that transfers heat from multiple systems to the Heat Rejection System (HRS).
- Chilled Water System (CHWS): Provides cooling water to remove heat from client systems that require coolant temperatures lower (6°C) than can be provided by the CCWS.
- Heat Rejection System (HRS): A tertiary loop that dissipates heat from both nuclear and non-nuclear components into the environment.

The Tokamak Cooling Water System (TCWS) (Fig. 3.1) is the largest and most critical of all systems and is the sole focus of this study. Its primary function is to evacuate heat from the Vacuum Vessel (VV), in-VV components (blanket modules, divertor, in-VV coils, etc.), and the Neutral Beam Injector (NBI) while maintaining coolant temperatures, pressures, and flow rates. The evacuation must occur both during plasma operation and decay heat removal.

The TCWS shares significant similarities with other power plant cooling loops. However, nuclear fusion imposes several unconventional requirements on the system. TCWS must supply water baking to the vacuum vessel (VV), in-VV components, and the neutral beam injector (NBI), which is essential for removing impurities and residual gases that could contaminate the plasma, such as hydrogen and deuterium. Additionally, the system provides hot nitrogen gas for blow-out of in-VV components, drying of the VV and in-VV components, and divertor gas baking. Furthermore, the TCWS must ensure primary confinement of activated corrosion products (ACPs) and tritium entrained in the cooling water outside the VV while maintaining leak-tight integrity in all system states.

To meet all design requirements and nuclear safety objectives, the TCWS team developed a system that is, in many ways, novel and first-of-its-kind. Although the system's components and operation are technically interesting, they have little relevance to the design task, with the exception of nuclear valves.

[1] ELM (Edge-Localized Modes) control systems help stabilize plasma and prevent damage from sudden energy bursts.
[2] NBI is used to heat the plasma by injecting high-energy neutral particles, generating a significant heat load that needs cooling.

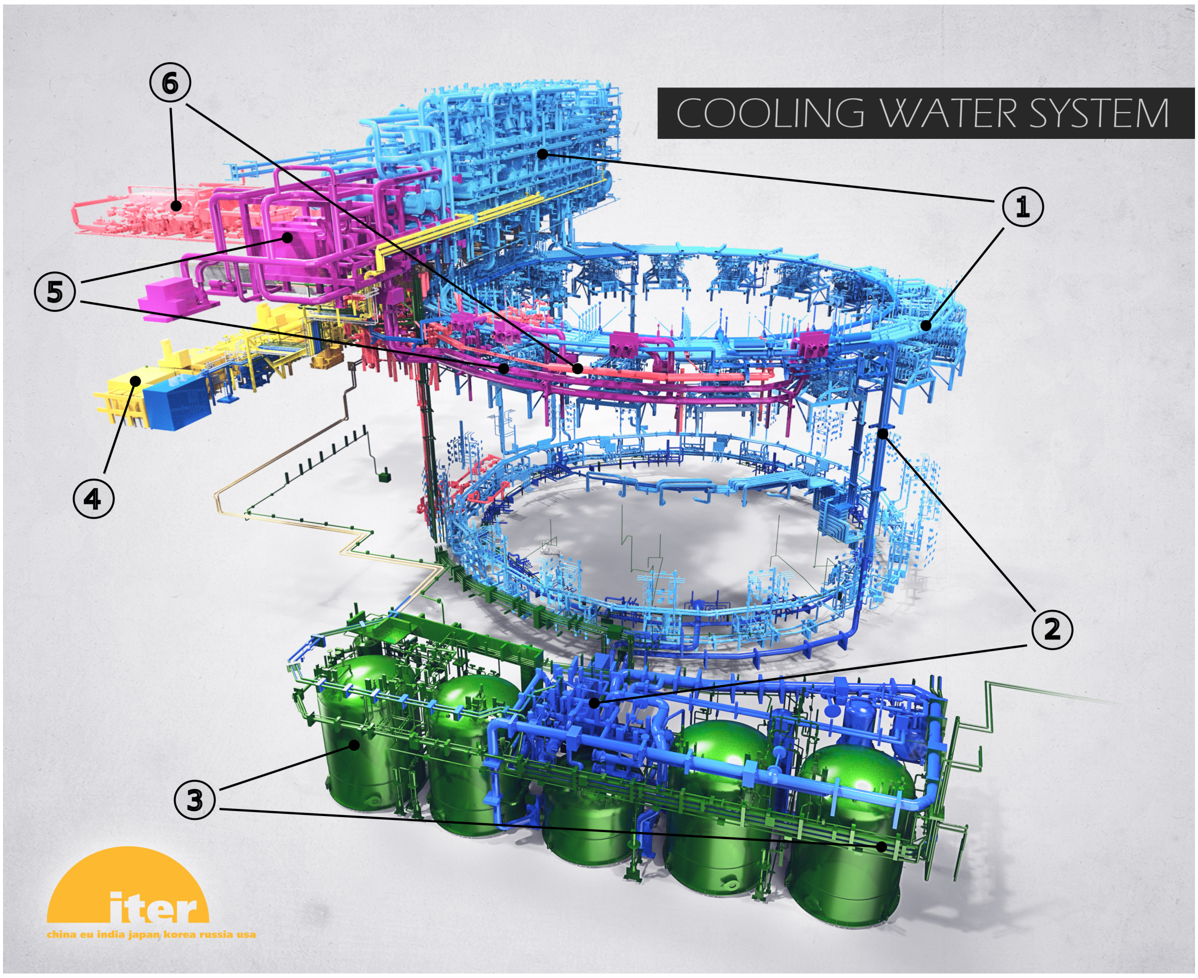

Figure 3.1: The Tokamak Cooling Water System (TCWS). Parts: (1) IBED - Integrated Blanket, ELM and Divertor Cooling, (2) VV - Vacuum Vessel Cooling, (3) Draining (4) Chemical and Volume Control System, (5) Neutral Beam Injector Cooling (6) Drying. Source: [9], modified by Marcell Szabo, 2025.

3.2. TCWS valves

TCWS valves distribute and control water while ensuring safety functions in designated areas. They control the flow of water throughout the whole TCWS system, making their operation required for both safety-critical and standard operational scenarios. Although these valves are not the thesis' primary focus, their description is important to understand the design task. TCWS valves can be classified into two sub-groups based on whether they need rotary or linear motion to open and close.

Rotary motion is generally needed by ball and butterfly valves. Ball valves (Fig. 3.2a) make use of a ball with an opening rotated by the valve stem. They give a tight shutoff while opening quickly when needed. When fully open, they provide little to no turbulence or resistance to the flow. On the other hand, in butterfly valves (Fig. 3.2b), a disc is used to obstruct the flow by rotating the attached shaft with a bearing. These are also high recovery valves, since only the disc obstructs the flow. However, they have the added advantage of flow regulation. [13]

Linear motion is common for globe valves (Fig. 3.2c). This type consists of a moveable plug- or disk-like element that can sit on a stationary ring. It is mostly used in throttling applications and has a low recovery rate (high obstruction of flow, big pressure drops, low flow rates). The globe and seat construction gives the valve good flow regulation characteristics.

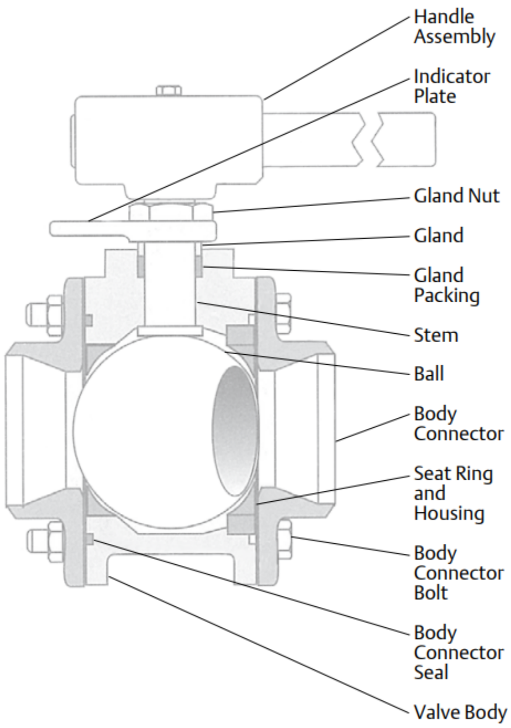

(a) Reduced-port ball valve. Ball valves make use of a ball with an opening rotated by the valve stem.

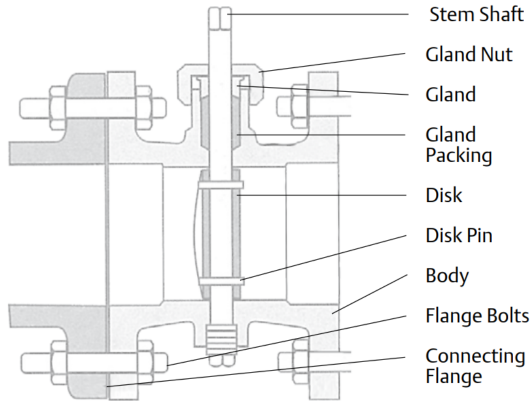

(b) Butterfly valve. In butterfly valves, a disc is used to obstruct the flow by rotating the attached shaft with a bearing.

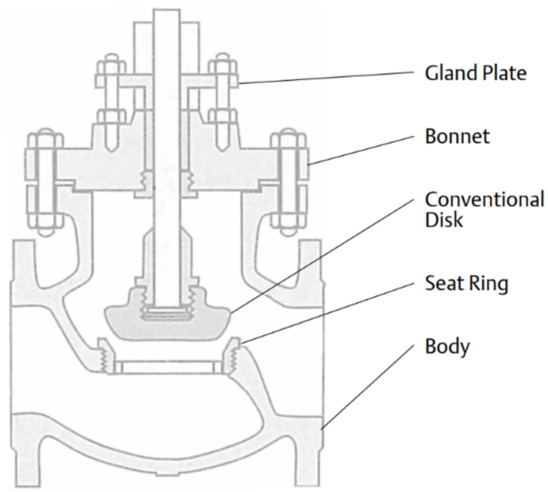

(c) Conventional disk globe valve. This type consists of a moveable plug- or disk-like element that is moved vertically to throttle the flow.

Figure 3.2: Relevant valve types for the design task. Source: [14]

Throughout a single plasma cycle, the TCWS must perform multiple functions, such as water baking, coolant circulation, and gas blow-out. Each of these requires rapid and reliable valve operation, provided by actuators. Actuators produce force to move the valve into a desired position, mostly via remote control in nuclear power applications. Their most common types are electric and pneumatic actuators [13]. Both have advantages and limitations, but at ITER, magnetic fields are the determining factor. When using electric actuators next to the tokamak, the magnets' static magnetic field disturbs the operation of all electric and magnetic components. Although magnetic shielding offers a solution, it is preferred to use mechanical systems to avoid all magnetic issues. Hence, ITER uses pneumatic actuators to command all valves.

These actuators are primarily selected based on the corresponding TCWS actuated valve's required motion.

Their fail-safe principle ensures that the reactor and associated systems automatically transition to a safe state in the event of a failure, power loss, or malfunction. Pneumatic actuators apply air pressure to move the valve stem. When pressure is lost, these actuators move the valve into a pre-determined position, defined by the process engineer, thereby achieving fail-safe functionality. Consequently, numerous pneumatically actuated control and nuclear safety valves are used within the TCWS. Since these require compressed air, an auxiliary compressed air system must be implemented. This system, designated PBS26.CATC (Plant Breakdown System Nr. 26 (CWS), Compressed Air for Tokamak Cooling), is the subject of this thesis work and is introduced in the following chapter.

4

The Compressed Air System

4.1. Pneumatic Actuators

To prepare for potential incidents, ITER has conducted safety evaluations for each specific incident type, defining safety functions to mitigate their effects. These include airplane crashes, earthquakes, fires, and external explosions [15] [16]. TCWS valves utilise pneumatic actuators to provide fail-safe operation in case of such an event, necessitating the implementation of the 26CATC compressed air system, designed in the thesis work. By comparing fail-safe mode with valve position during plasma operation, an appropriate design can be proposed for each valve [17] [18]. Within the TCWS, actuated valves can assume one of three fail-safe positions:

- Fail Open (FO): these valves request compressed air to be closed and are normally opened by a spring when air is removed from the air chamber.
- Fail Close (FC): these valves request compressed air to be opened and are normally closed by a spring when air is removed from the air chamber.
- Fail in Position (FP): these valves request compressed air to be either open or closed. They only rely on compressed air during operation (e.g. no spring is used in their actuator bodies) and they remain in their last operating position in case of supply loss.

Although the design requirements are well-defined, the specific pneumatic actuator types have yet to be determined. Depending on the required motion, the TCWS employs diaphragm actuators for linear motion and rack-and-pinion actuators for rotary motion. While both types can be adapted to provide either movement through appropriate design modifications, considerations such as simplicity and space constraints typically dictate the selection.

Linear diaphragm actuators can be either single-acting or double-acting. Within the TCWS, they are used for globe valves responsible for flow control, necessitating only the double-acting configuration. These employ a springless design in which the diaphragm can be actuated by air pressure from both sides (Fig. 4.1).

Rotary rack-and-pinion actuators can be either double-acting or spring-return. In TCWS, spring-return actuators (Fig. 4.2) use air pressure to push against a spring-supported piston, which rotates the central pinion via a rack. The double-acting configuration (Fig. 4.3) eliminates the spring and operates with air pressure on both sides of the piston.

It is important to emphasise that different fail-safe operations require specific actuator actions. For FC or FO valves, a spring must ensure the correct fail-safe position upon air supply loss, making single-acting actuators the only viable choice. Conversely, FP valves must keep the pistons and racks in position during a failure, necessitating a springless design and a double-acting configuration. For the TCWS, multiple actuator suppliers have been selected based on valve type (motion type, thrust, and travel distance), nominal diameter (DN), and ASME[1] class.

[1] American Society of Mechanical Engineers

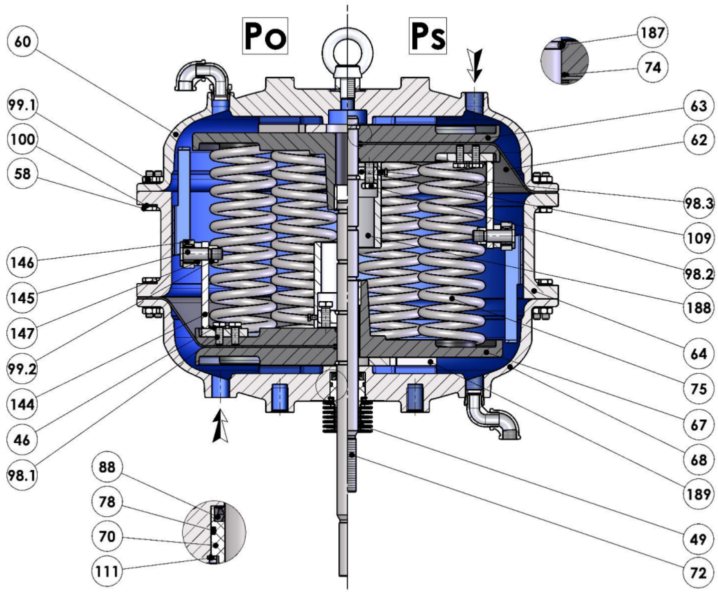

Figure 4.1: Single-acting linear diaphragm pneumatic actuator design. Reverse-acting (left) and direct-acting (right) configurations. During pressurzation, air is supplied through *Ps* and the diaphragm is pushed against the spring. When pressure from *Ps* side is lost, the spring pushes the diaphragm into the opoosite position, venting the air through *Ps*. Source: [19] *Note: Double-acting diaphragm actuator was not found in public sources. Drawings are available in [20] for such a design. However, third-party intellectual property disclosure is not allowed, therefore a single-acting design is displayed. The double-acting design does not use springs on either side.*

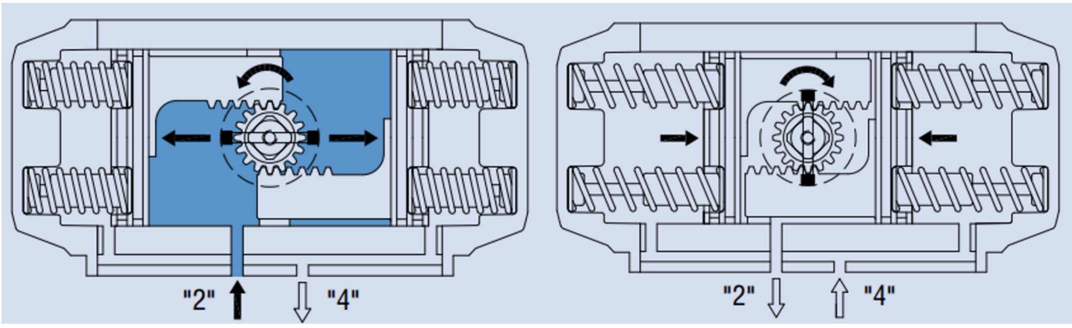

Figure 4.2: Single-acting rotary piston actuator operation scheme. When pressurized from Port "2", compressed air pushes against the spring-supported piston, rotating the central pinion and the attached valve stem via a rack. When pressure from Port "2" is lost, the spring pushes the rack back, turning the pinion in the opposite direction and venting the air through "2". Source:[21].

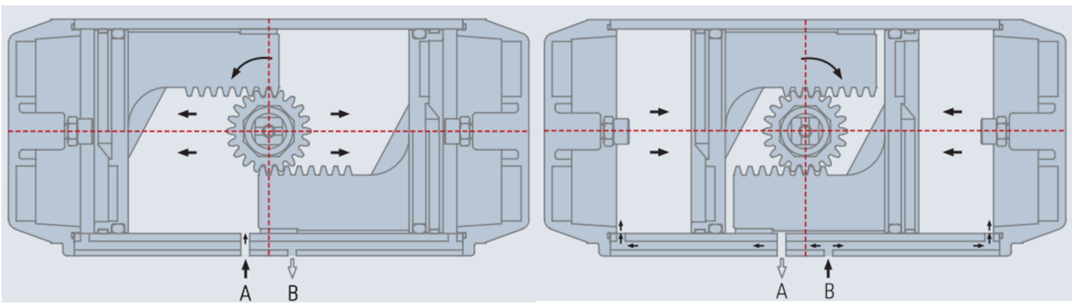

Figure 4.3: Double-acting rotary piston actuator operation scheme. Pressurization happens from both "2" and "4", depending on the movement required. The air enters the central or outside chamber and pushes the pistons out (center) or in (outside), turning the central pinion in the respective direction. Source:[22]

4.2. Pneumatic Control

To control these actuators, pneumatic systems use solenoid valves (SV) to supply and remove compressed air. Their working principle is shown in Figure 4.4. A SV is a type of valve actuated by an electric current passing through a circular coil (8) that surrounds a cylindrical steel core and/or plunger (9,10). This current creates a magnetic potential difference across the air gap, generating an attractive force that moves the plunger, thereby opening or closing the valve [23]. At ITER, solenoid valves control airflow to the pneumatic actuator chambers, regulating their operation. The energizing current is supplied by the control device responsible for executing operational and safety functions. Since for remote control the use of solenoid valves is inevitable, ITER uses magnetically shielded solenoid boxes to protect their functionality from the tokamak's static magnetic fields.

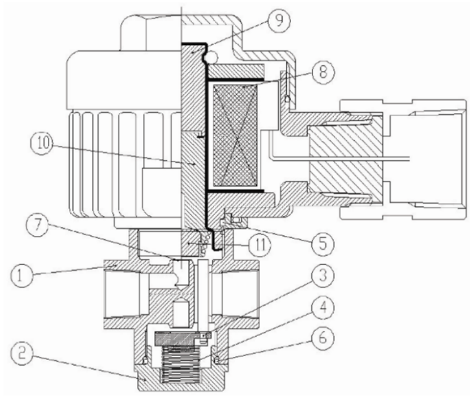

Figure 4.4: Solenoid valve configuration. An electric current passes through a circular coil (8) that surrounds a cylindrical steel core and/or plunger (9,10). This current creates a magnetic potential difference across the air gap, generating an attractive force that moves the plunger, thereby opening or closing the valve. Source:[23]

Solenoid valves are connected in various configurations to provide precise functionality for each TCWS valve. The two general control types are Direct Control (DC, presented below) and Piloted Air-Operated Valve (Piloted AOV, presented in two configurations in Appendix A) [24]. Depending on the required fail-safe action, Piloted AOV configurations can be applied to Fail Open (FO), Fail Close (FC), or Fail in Position (FP) valves. More sophisticated control types are not feasible due to the stringent fail-safe requirements and the harsh environment inside the Tokamak Building (strong magnetic field, radiation exposure).

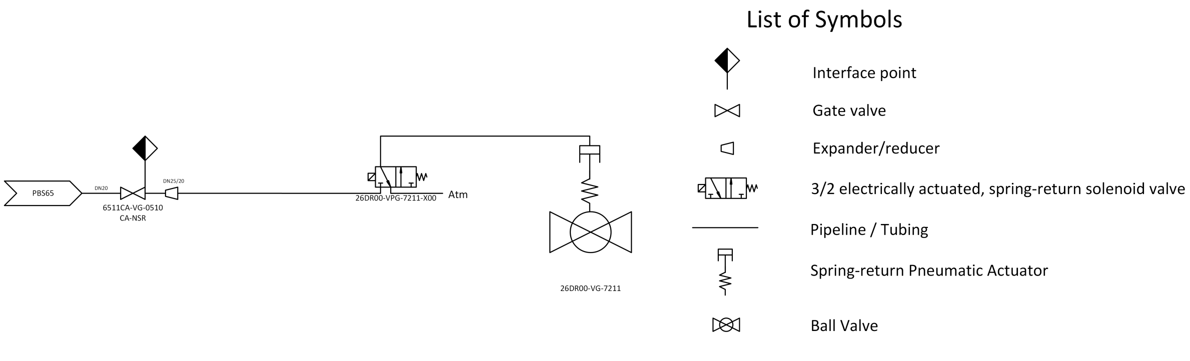

Figure 4.5: Schematic diagram for solenoid valve function for DC.

Direct Control

Direct Control (DC) employs a 3/2 solenoid valve directly connected to the compressed air supply. Figure 4.6 schematically illustrates the routing. When the solenoid valve is energized, compressed air from Liquid & Gas Distribution System (PBS65.CA) is directed to the actuator. The flow passes through a Flow Control Valve (FCV) regulating the flow rate, and a Quick Exhaust Valve (QEV) to reach the actuator inside chamber. The pressure then opens FC, and closes FO valves. In the event of de-energization or system failure, pressure is lost from the supply line. The remaining air from the inside chamber vents through the same QEV and is regulated by the other FCV, as the spring pushes the racks back. As a result, FC valves close, FO valves open, and when applicable, fail-safe mode is achieved. The specific roles of FCVs and QEVs are discussed later in the Appendix A.

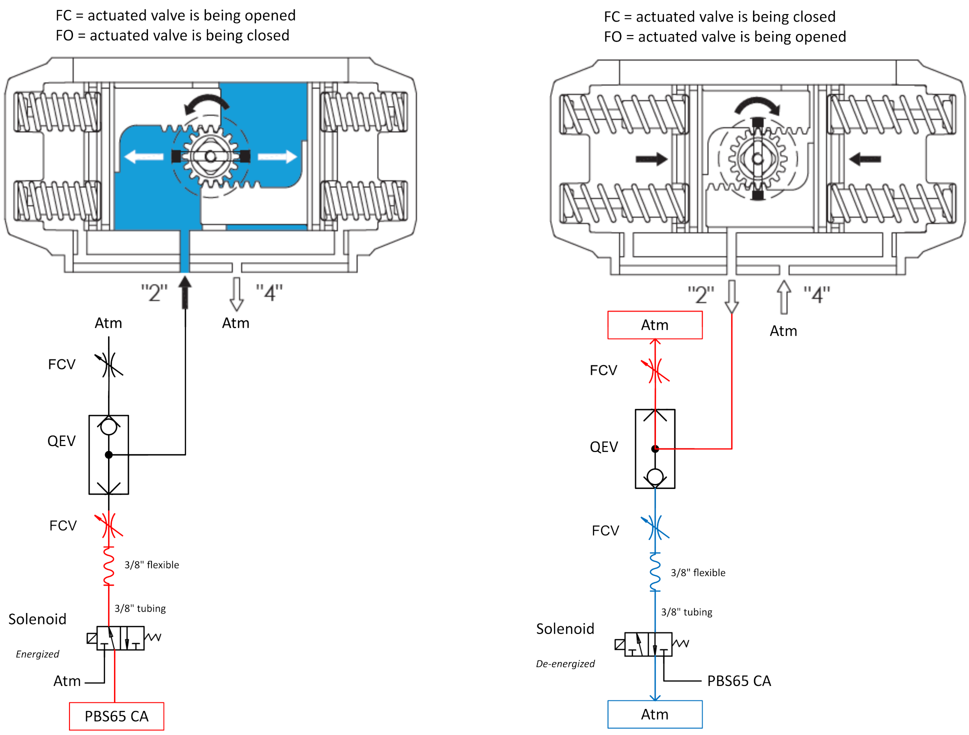

Figure 4.6: Direct Control configuration for FO or FC valves. When SV is energized (left), compressed air from PBS65.CA is directed to the actuator. The flow passes through an FCV and a QEV to reach the actuator inside chamber (Port ”2”). The pressure then moves the piston against the springs. During de-energization (right), pressure is lost from the supply line. Air vents through Port ”2”, the same QEV, and the other FCV, as the spring pushes the racks back. Source: [25], modified by Marcell Szabo, 2025.

However, the DC configuration presents two issues. Firstly, the compressed air passes through a line of accessories leading to higher hydraulic resistance and lower air flow rate. As a result, a noticeable delay occurs in the actuators' stroke times. Stroke times are important for general system responsiveness and operation, and are also defined in [18]. When the stroke time is not achieved by DC, a 3/2 Piloted Air Operated Valve (Piloted AOV) configuration is proposed to shorten the supply line.

Additionally, achieving FP double-acting motion requires supplying compressed air to two separate ports. This can only be accomplished by implementing two solenoid valves – one closing and one opening the actuator – along with a 5/3 Piloted AOV to control the flow and provide fail-safe action.

While the exact routing layout is an essential design aspect, it does not provide significantly more insight beyond the explanations above. Therefore, it is discussed in Appendix A, along with other network components used for controlling, throttling, and directing airflow to, or from the actuator.

5

Design Goals

Compressible flow modelling in nuclear systems is a highly unconventional exercise. Nuclear power plants often operate with a large number of Air Operated Valves (AOVs), and Solenoid Operated Valves (SOVs) can number in the thousands in certain reactors. While pneumatic systems vary across plants, most designs separate safety-related AOVs from conventional ones. Safety-related valves are typically backed up by pneumatic accumulators—pressure vessels located near the valve—to ensure reliable operation if the central air supply is lost. ITER, however, presents unique challenges. All auxiliary plant systems are placed outside the cryostat, which creates significant spatial constraints within the already-built Tokamak Building. To overcome this, ITER engineers designed a centralised compressed air system, with safety valves supplied by a dedicated compressor station. This approach eliminates the need for local accumulators but introduces a new challenge: ensuring that valves remain operable despite being several hundred meters from their air source. In practice, operability means respecting stroke times. In the Cooling Water System, each valve has a specified stroke time range for opening and closing. For instance, valve 26PHBD-VG-1905 is an in-vessel LOCA (Loss of Coolant Accident) valve that must close within a strict timeframe if a pipe break occurs. Safety engineers therefore assigned stroke time requirements to the 26CATC network, in this case between 10 and 12 seconds. Verifying that valves meet these limits is critical, as all subsequent thermal-hydraulic analyses rely on these timings as input for nuclear safety assessments. This is the first design goal, detailed in Section 6.1.

To assess whether closing the valve in time is possible, modelling fluid flow along the compressed air layout is essential. This requires dedicated software: solving compressible flow equations across complex layouts cannot be done by hand, especially given the safety-critical nature of equipment operation. The chosen software is AFT Arrow by Applied Flow Technology — a steady-state compressible flow modelling code verified for nuclear applications [26]. The general working principle and the sofware verification is described in Appendix B. It is important to note that the version used in this study can only solve equations for time-independent flows, a phenomenon rarely present in the ever-moving system of ITER's cooling water valves.

To accurately model the physics during operation, it is necessary to understand the loading effects and system logic. Pneumatic actuators must open and close under different loading conditions, which require different pressures to overcome. This directly relates to the Arrow models' boundary conditions: the higher the load, the higher the required pressure, reducing the available pressure drop Δp between the compressor station and the actuator chamber. This lowers the mass flow rate into the chamber and increases the stroke time. The physics of operating pneumatic actuators and the underlying load assumptions are detailed in Section 6.1.1, along with the method used to set the boundary conditions.

Another important aspect is the hydraulic resistance of the piping leading to the actuator chamber. Significant effort was made to obtain the piping isometrics and the resistance of individual fittings (see Appendix A). The goal was not only to model the isometrics as they are, but also to develop a method for quickly reassessing stroke times if the layout changes later in design. This is summarised in Section 6.1.2, which also describes the model settings, such as accounting for compressibility or heat transfer effects.

Finally, the most important step is to create model scenarios that evaluate compressed air demand when several valves are actuated at once. When valves operate simultaneously, the pipe network can only supply a finite amount of air depending on its layout and the required pressures, which can lead to longer stroke times. The logic for defining the scenarios and the final method is described in Subsection 6.1.3. After running the Arrow models, a single mass flow rate ($\dot{m}$) is obtained for each valve, which can then be compared to the set requirements.

However, this only demonstrates stroke time compliance. If the Arrow models show that the theoretical stroke times do not exceed the maximum value (for 26PHBD-VG-1905, the defined 12-second constraint), then operability is verified in all relevant conditions. This marks a necessary, but not sufficient, step in the design. It is also essential to verify whether the Compressed Air Supply can provide the required amount of air. This is the second design goal, further discussed in Section 6.2.

For demand calculations, the Arrow models do not provide accurate mass flow rate estimates. The 26CATC network includes several FCVs (Flow Control Valves), which are used during commissioning to throttle flow and increase stroke times, a measure necessary to avoid undesired water hammer effects. As a result, peak consumption differs from Arrow predictions.

Lastly, the issue of system overpressure is addressed. The upstream network (PBS65) connects to the 26CATC network through 61 interface points distributed inside the Tokamak Building. This central compressed air network serves as the source for all distributed air across ITER, so the supply pressure must meet the demands of various systems throughout the plant. This results in a declared static pressure range of $7\,\mathrm{barg}$ to $11\,\mathrm{barg}$ at the interface point. However, the downstream actuators have a much lower maximum allowable pressure. To ensure a sufficiently long lifetime and for economic and nuclear safety considerations, actuator protection is necessary. For this, PRVs (Pressure Reducing Valves) are proposed. The sizing of these valves depends strongly on the peak consumption calculation, since undersized devices can choke the network. Furthermore, their hydraulic resistance shall also be considered when verifying the stroke times, making an iterative process necessary. Their sizing, pressure setting, and placement are described in Section 6.3.

In conclusion, the identified design goals are the following:

- Verify stroke time requirements
- Calculate compressed air consumption
- Size Pressure Reducing Valves to protect the network from overpressure

A schematic diagram is shown in Figure 5.1 to illustrate the sizing calculation process. The sizing starts with the Stroke Time Verification Calculation, which evaluates whether the required pneumatic stroking times are achievable. Once this is done, the focus shift on the Compressed Air Consumption Calculation, which evaluates whether the compressor station will be able to supply the peak and continuous consumption of the network. In case of failing to meet stroke time or demand requirements, the re-evaluation of the current design is advised. The third and last step of the process is the PRV Sizing, which uses the flow rates calculated in the Consumption Calculation as a sizing input. Once the sizing is complete, the PRVs need to be included into the AFT Arrow models again, which is then used to re-calculate the pneumatic stroking times of the system. Although this thesis report aims to present the processes in a simple yet thorough manner, the author acknowledges that the described methods may appear theoretical and abstract. Because this work focuses on generating a new design, the methods are demonstrated through a worked example. This example is used throughout the report to help explain and visualize the complex system under study.

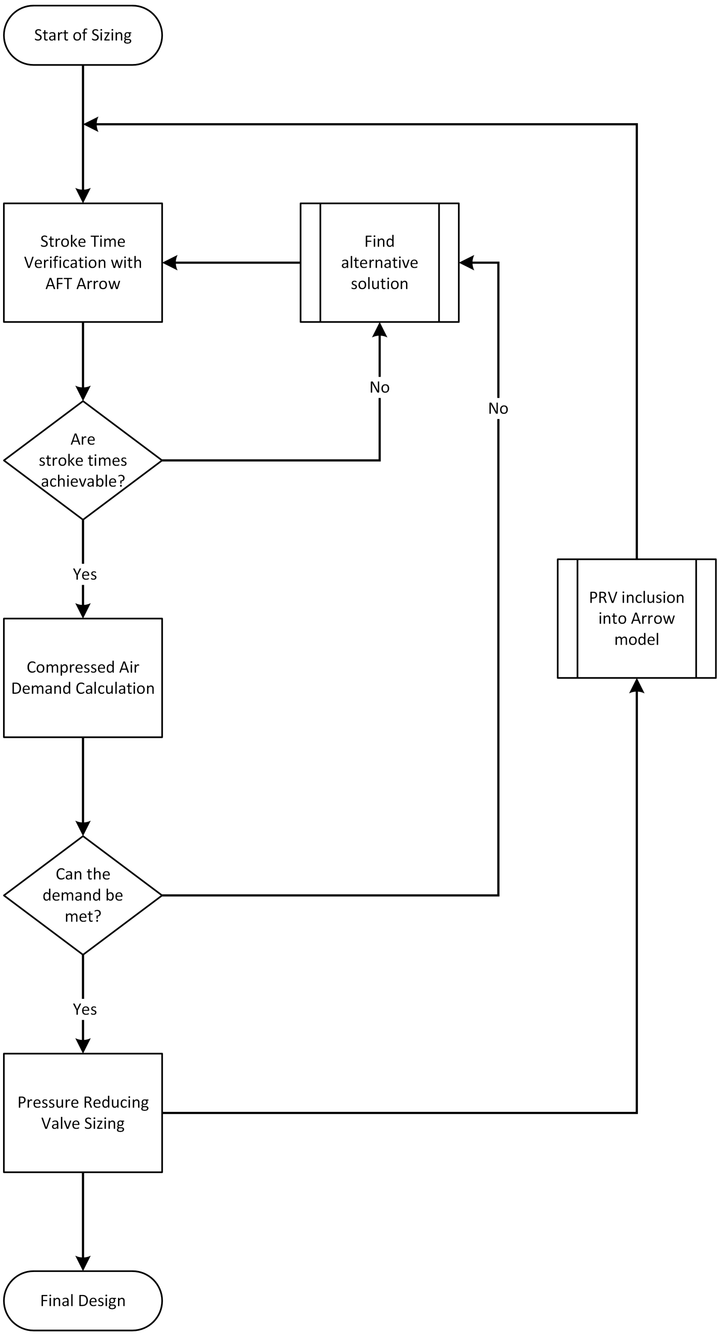

Figure 5.1: Thesis workflow. The study starts by the Stroke Time Verification Calculation, evaluating whether the required pneumatic stroking times are achievable. Then comes the Consumption Calculation, which evaluates whether the compressor station will be able to supply the peak and continuous consumption of the network. In case of failing to meet stroke time or demand requirements, the re-evaluation of the current design is advised. The third and last step of the process is the PRV Sizing, which uses the flow rates calculated in the Consumption Calculation to size the reducers. Once the sizing is complete, the PRVs need to be included into the AFT Arrow models again, which is then used to re-calculate the pneumatic stroking times of the system.

6

Design Method

6.1. Stroke Time Verification Calculation

Stroke time verification forms the backbone of this study. Without confirming the valves' ability to operate within the required time interval, all dependent thermal-hydraulic and sizing calculations become invalid. To verify that the required stroke times are achievable, the determining factors must first be identified. However, it is important to highlight in the very beginning that the hereby process describes the stroke time calculation for pressurisation cases - i.e. when the 26CATC supplies compressed air to open (for Fail Close or Fail in Position valves) or close (for Fail Open or Fail in Position valves) with the actuator. For the depressurization process of Fail Open and Fail Close actuators, the actuator supplier is responsible for conducting experimental tests and verifying the corresponding stroke times.

Pressurisation stroke times depend on numerous things. Firstly, they are dependent on the external load the actuators must move to open and close. This is shown with the equation of piston motion applied to pneumatic actuators [27]:

$$ma = P_1 \cdot A_1 - P_2 \cdot A_2 - F_f - F_L \tag{6.1}$$

where:

- m is the mass of the accelerated components, such as the piston and the load
- a is the acceleration
- P_1 and P_2 are the supply and exhaust pressures in the pressurised and de-pressurised chambers
- A_1 and A_2 are the effective areas of the respective chambers
- F_f is the friction force acting against the direction of movement
- F_L is the external force.

Equation 6.1 shows that the higher the external load (i.e. the process loading conditions on the valve), the higher the required P_1 supply pressure is. The higher this pressure, the lower the available pressure drop from the compressor station and the lower the mass flow rate filling up the chamber.

Secondly, the mass flow rates are also dependent on the hydraulic resistance of the network, which regulates how much flow can pass through the pipeline to the actuator chamber. Lastly, simultaneous demand must also be considered since this can decrease the mass flow rate entering the individual valves. The present study investigates these effects.

At this design stage, however, the available information is limited. For example, compressor capacity data is not yet available, making direct application of fluid power equations impractical. To address this, a new method has been developed to calculate stroke times, shown in Figure 6.1. The method uses AFT Arrow to model the mass flow rates within the network. The approach begins by defining the scope of the models, aiming to reflect the physical phenomena inside the network while keeping practical considerations in view. One such consideration is setting the simulation's boundary conditions, which is challenging at this stage given the limited data. Section 6.1.1 offers an approach which uses the available actuator load and calculates the chamber pressure needed to move it.

After laying these foundations, the method continues with building AFT Arrow models. The Process and Instrumentation Diagram (P&ID) [28] provides a basis for the simplified routing of the entire 26CATC network. Drawing these routes in AFT Arrow creates a base structure, into which input data such as pipe sizes, bend geometries, and valve resistances are later added. This is described in Section 6.1.2. Here, the network isometrics are collected from the already available 3D model in the form of geometric data. These are then converted into hydraulic resistance (such as K or C_V values) and - along with the resistances of the other network junctions - are imported into the AFT Arrow base structure.

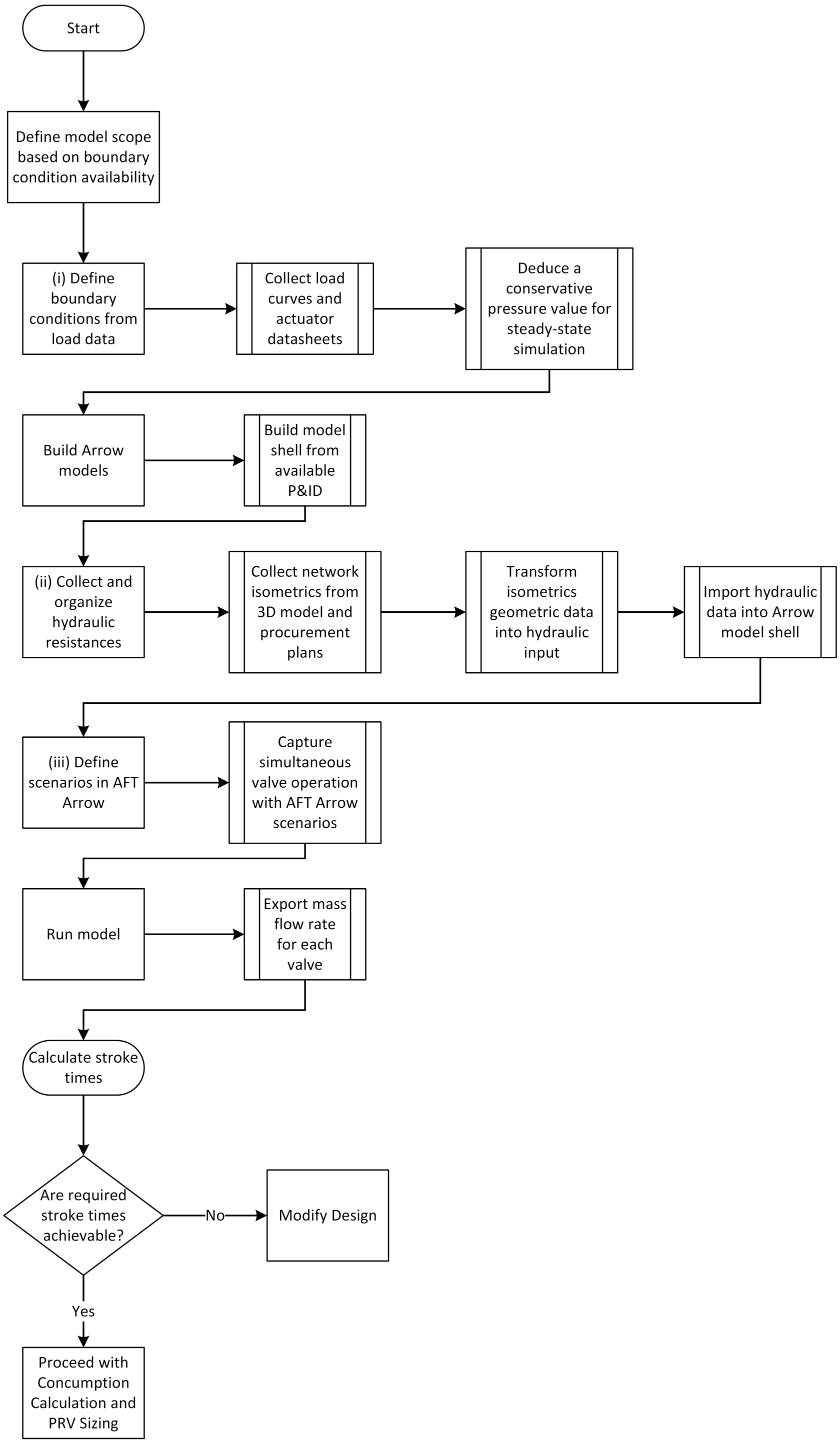

Figure 6.1: Developed method for stroke time verification. The method uses AFT Arrow models to calculate the forming mass flow rates between the interface point and the connected actuator chambers.

At this point of the process, the model scope, boundary conditions, and isometrics are all present. Therefore, only the operability considerations are missing. Section 6.1.3 shows how scenarios - a function of AFT Arrow - are defined to assess the forming mass flow rates during nuclear safety events or other likely operational conditions. Once this last step is taken, the model is ready to run and provide a mass flow rate value for each actuator in the network. Once these values are collected, the total stroking time T_3 is calculated and compared against the required stroke time. If the requirement is satisfied, the design can proceed with the Consumption Calculation (Section 6.2) and the PRV Sizing (Section 6.3). In case of failure, design modifications must be considered.

To better understand the applied method, a schematic is shown of the whole ITER Compressed Air Network on Figure 6.2. It is important to note that on the real network, the number of subnetworks and actuators is much higher than on the presented drawing. In the studied compressed air system, the fluid flow originates from the compressor station (1), travels through a long journey with several junctions dividing the flow (2), until it arrives at the interface points (4) at several different locations. Since the Compressed Air Supply is a central supplier to several clients, these interface points mean the boundary between the supplier and the specific client, such as the Tokamak Cooling Water System. The flow travels through a gate valve (3), after which the responsibility of design is delegated to the downstream engineering team - in this case, the author(s) of this report. The air then continues to travel to the specific actuator, flowing through various fittings that provide control functions but also contribute to additional pressure losses. Figure 6.2 depicts three lines: the upper line is often referred to as ”Direct Control”, since here the actuator (9) is fed directly through the commanding Solenoid Valve (6). This solenoid is normally closed, and will be opened remotely via an electric system controlled by the central Operation Room when commissioned. Once opened, the air passes through the Flow Control Valve (7), which allows throttling, and the Quick Exhaust Valve (8), which ensures rapid venting of the actuator chamber when the solenoid closes again. Finally, the air reaches the actuator chamber (9) and acts against the fluid flow inside the TCWS valve (11). While simple, this design has limitations: it is unsuitable for double-acting actuators and the long tubing between the solenoid and flow control valve increases hydraulic resistance. To overcome these difficulties, two subsequent designs utilizing Piloted Air Operated Valves (Piloted AOVs) are implemented: one for double-acting Fail in Position (FP) actuators (middle line) and one for Fail-Open/Fail-Close (FO/FC) actuators (bottom line). FP actuators make use of a 5/3 AOV (13) commanded by two separate solenoid valves (6) to achieve the desired movement, while FO/FC actuators use 3/2 AOVs (12) to get a direct supply from the 26CATC network without the solenoid valve (6) slowing the flow. The three layouts together cover all possible command modes in the 26CATC network, and therefore provide a complete basis for further discussion.

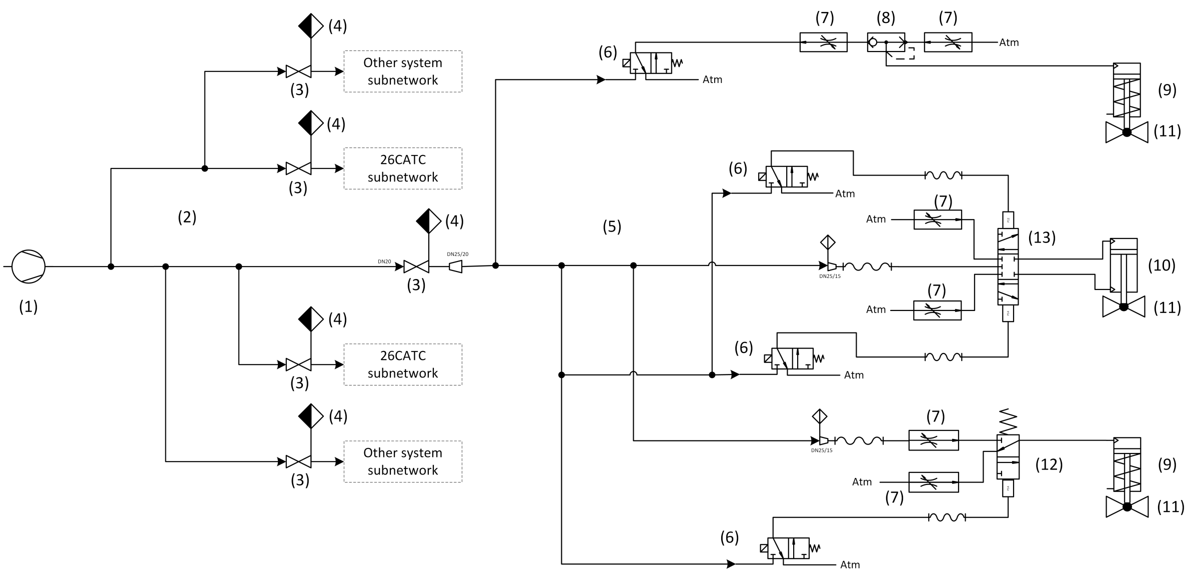

Figure 6.2: Schematic diagram of the ITER Compressed Air Network. (1) Compressor Station, (2) Compressed Air Distribution System, (3) Gate Valve, (4) Interface Point, (5) 26CATC, (6) Solenoid Valve, (7) Flow Control Valve, (8) Quick Exhaust Valve, (9) Single-Acting Pneumatic Actuator, (10) Double-Acting Pneumatic Actuator, (11) TCWS Valve, (12) 3/2 AOV, (13) 5/3 AOV

As stated above, as a first step in the design, the required stroke times need to be verified. In practice, this means that the stroke times calculated need to be lower than the maximum required value of the time interval. If the stroke times cannot be verified, the layout must be changed or redesigned. On the contrary, if the calculated stroking time is below the minimum requirement, Flow Control Valves (7) provide means to increase the hydraulic resistance of the network, thereby extending the stroking time. Consequently, this section focuses on verifying that valves can open and close under the required maximum stroking time. For this purpose, simulations are carried out using AFT Arrow. Those will investigate the forming mass flow rate in worst-case conditions through the 26CATC network. Once the simulations are run, the software will calculate a single flow rate, which can be used with the known actuator volumes to calculate the pneumatic stroking times. As a first step to build the necessary AFT Arrow models, the boundary conditions are discussed.

6.1.1. Actuator loads - boundary conditions

To determine the boundary conditions, the first step is to define the modelling scope. Ideally, the model would start at the compressor station, but ITER's centralized compressed air structure makes this impractical. The upstream side of the interface point is designed by a different engineering team, meaning that information such as compressor curves, upstream isometrics, and the consumption of other networks is not directly available to the authors. To simplify the task, an interface sheet has been created by the upstream team to convey information to all clients [29]. This document provides the most important available data at the interface point, such as pressure and flow rate, effectively splitting the network into two separate parts. Specifically, the declared static pressure ranges from $7\,\mathrm{barg}$ to $11\,\mathrm{barg}$ on the supply side. Due to this constraint, it is most convenient to start building the AFT Arrow models from the interface point.

For each interface, a new model is created with the interface sheet's declared pressure used as the upstream pressure boundary condition. Since the design aims to verify stroke times under worst-case conditions, the minimum declared pressure of $7\,\mathrm{barg}$ is applied. This creates the lowest possible pressure drop (Δp) between the interface and the actuator chamber, which in turn minimises the mass flow rate. As a result, the calculated stroke time is conservatively maximized, representing the slowest possible valve response.

Continuing downstream, the air flow passes through various fittings and junctions until it reaches its final destination - the actuator chamber. Here, the compressed air flows through an inlet port, enters the chamber, and gradually moves the actuator into the desired position. Since the air does not leave the chamber until further command, it becomes a convenient place to set as the Arrow model's downstream boundary. However, it is not clear at this point what the boundary condition for the chamber is. AFT Arrow offers two types of boundaries: pressure and flow. Flow boundaries are common to use when an experimental flow rate measurement is available. This is untrue for the ITER Compressed Air network, since the system is still in the design phase and has not yet been installed. For this reason, applying a pressure boundary is the more practical and realistic option. By declaring an upstream and a downstream pressure, the model can calculate the developing mass flow rate. However, the chamber pressure is heavily dependent on the actuator's load, which in turn comes from the cooling water's mechanical load on the valve. A higher value means a higher required torque/force from the actuator, which increases the required pressure in the actuator chamber. This will then minimise the available pressure drop Δp between the interface point and the actuator, decreasing the mass flow rate and increasing the stroke time. Therefore, it is important to use a pressure boundary which provides a conservative estimation of the stroke times.

The estimation of the pressure boundaries was done by analysing the available load calculations for each actuator [30]. An example of the results for such a calculation is shown in Figure 6.3a: during the specific actuator's opening, the required torque is calculated for eight discrete points, each corresponding to a different opening angle. This suggests that the actuator chamber pressure will vary significantly as the load drops more than 50% during opening. This is highly inconvenient, since AFT Arrow can only solve steady-state problems with constant pressures used as boundary conditions. To help Arrow simulations, the goal is hance to determine a single conservative pressure boundary.

This is done by using valve calculation notes (e.g., Figure 6.3a) and actuator datasheets (Figure 6.3b). Calculation notes provide the torque and force curves depending on the valve and actuator type [30]. On the other hand, actuator datasheets provide torque-pressure and force-pressure diagrams [31]. This allows to convert the required load values into chamber pressures. However, this still results in a pressure curve following the loads during stem movement. To deduce a single conservative pressure value for a boundary condition, the highest required load value (excluding the first point) was taken. This is due to the fact that some non safety related valves require $7\,\mathrm{barg}$ to open at the very beginning. If this was taken as the boundary downstream, the Arrow model would end up having the same pressures on both ends. To reduce conservativeness and allow modelling these valves, the second pre-calculated point was taken, and the corresponding pressure was read from the actuator datasheets. The problem of opening the non safety-important valves has been raised as an issue to the 26CATC engineering team and is also discussed in Chapter 8. For safety important valves, the valve sizing was conducted with 5 barg supply pressure, ensuring valve opening 2 bar lower. To remain conservative for all non safety-important valves too, if the required supply pressure was found to be below 5 barg, the downstream boundary condition in the Arrow model was raised to 5 barg. This reduces the available Δp in the simulation and increases the calculated stroke time.

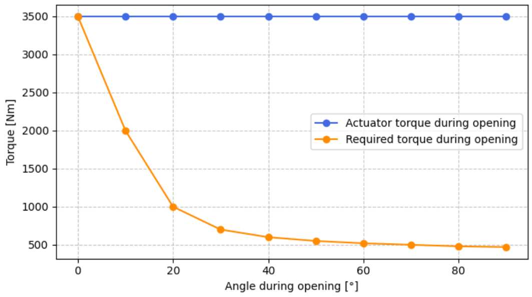

(a) Torque curves of DN300 butterfly valves using a double-acting actuator at 7 barg.

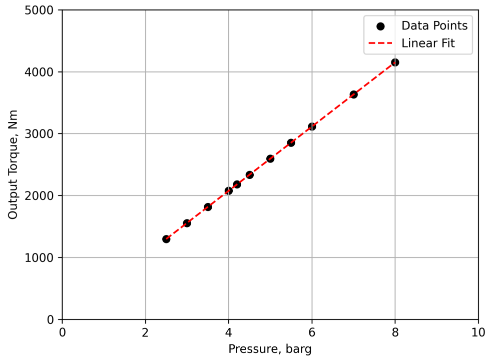

(b) Exerted torques of a double-acting actuator for different supply pressures.

Figure 6.3: Comparison of torque characteristics and actuator performance under varying supply pressures.

Deducing a single value for the actuator boundary conditions is useful for simplifying the subsequent calculations. When considering pneumatic actuators, stroking time can be divided into two parts: the *Latent* phase and the *Active* phase [25], [27]. The *Latent* phase includes the delay explained by the solenoid valve's reaction time and the pneumatic line length; as well as the actuator chamber dead volume pressurisation time to start opening the valve. This interval is denoted at ITER as T_{3a}—the time delay before actuator stem movement. The *Active* phase starts when piston displacement begins, and the rod accelerates to a finite velocity. This phase is denoted by T_{3b} at ITER, and ends when the rod reaches its endpoint and motion ceases.

A calculation already exists for the solenoid and pilot delays for each command type [25]. However, the time needed to pressurize the tubing and dead volume, as well as to completely fill the chamber for T_{3b}, still needs to be determined using the Arrow models. To calculate this, the single-chamber pressure derived from the torque curves is used. After the solenoid and pilot delays, it is assumed that the tubing, dead volume, and chamber are pressurized to the required pressure using the flow rate predicted by AFT Arrow, with this pressure set as the boundary condition. This assumption provides a conservative estimate—both by slightly underestimating the flow rate and by giving a cautious upper limit for the total mass of air needed to fill the volume.

To demonstrate this process with a specific example, the method is applied to one of the 61 26CATC interface points: 6511CA-VG-0511. This interface point connects 23 valves, for which the actuator types, fail-safe positions, stroke time requirements, and safety considerations are already defined [25], [18]. Based on the actuator types and the related calculation notes, the resulting actuator chamber boundary conditions are summarized in Table 6.1.

Table 6.1: Pressure Boundary Conditions for each actuator chamber at interface point 6511CA-VG-0511

Valve ID	Safe Failure	Actuator	Stroke Time Requirement	Boundary Condition Pressure, barg
26CCC1-VC-2513	FP	AT651U-D	[20s, 30s]	5
26CCC1-VC-2523	FP	AT651U-D	[20s, 30s]	5
26DR00-VC-1302	FP	MA41	[25s, 30s]	5
26DR00-VG-1304	FC	AT451U-S11	[15s, 30s]	5.3
26DR00-VC-4000	FP	AT351U-D	[25s, 60s]	5
26DR00-VG-4001	FC	AT451U-S11	[15s, 30s]	5.3
26DR00-VG-4008	FC	AT451U-S11	[15s, 30s]	5.3

Continued on next page

Valve ID	Safe Failure	Actuator	Stroke Time Requirement	Boundary Condition Pressure, barg
26DR00-VG-5000	FC	AT501U-S08	[25s, 30s]	5
26DR00-VG-5009	FC	AT451U-S11	[15s, 30s]	5.3
26DR00-VG-7313	FC	AT601U-S10	[25s, 60s]	5
26DR00-VG-9309	FC	AT501U-S10	[25s, 30s]	5
26PHVV-VC-1004	FP	AT701U-D	[20s, 30s]	5
26PHVV-VC-2002	FP	AT651U-D	[20s, 30s]	5
26PHVV-VC-3002	FP	PA60	[20s, 30s]	5
26PHVV-VG-1007	FP	AT1001U-D	[20s, 50s]	5
26PHVV-VG-9012	FC	AT601U-S10	[25s, 30s]	5
26PHVV-VG-9207	FC	AT451U-S10	[15s, 30s]	5
26PHVV-VG-9919	FC	AT601U-S10	[25s, 30s]	5
26SA00-VG-6002	FC	AT251U-S08	[15s, 30s]	5
26SA00-VG-6006	FC	AT251U-S08	[15s, 30s]	5
26SA00-VG-6009	FC	AT251U-S08	[15s, 30s]	5
26SA00-VG-6072	FC	AT251U-S08	[15s, 30s]	5
26SA00-VG-6074	FC	AT251U-S08	[15s, 30s]	5

6.1.2. Modelling hydraulic resistances - AFT Arrow

At this point, the modelling scope and corresponding boundary conditions have been defined. The models extend from the interface points between the central supply and the actuator chambers for pressurisation cases, while for de-pressurisation, they include the line from the vented chamber to the atmosphere. A method for the boundary conditions has been introduced to estimate conservative mass flow rates accounting for ”worst-case” scenarios during peak loading conditions on the process (TCWS) side.

The next step is to create the Arrow model shells themselves. Figure 6.4 exemplifies a theoretical Arrow model for the 26CATC schematic. It depicts the modelled network section for pressurisation cases (from the interface point to the actuator chambers). The models start with the upstream static pressure boundary followed by the pipe network of the specific interface point. It is important to note that the tubes leading to solenoid valves controlling Piloted AOVs are not included in the model, since the time it takes to fill these tubes has already been estimated [25].

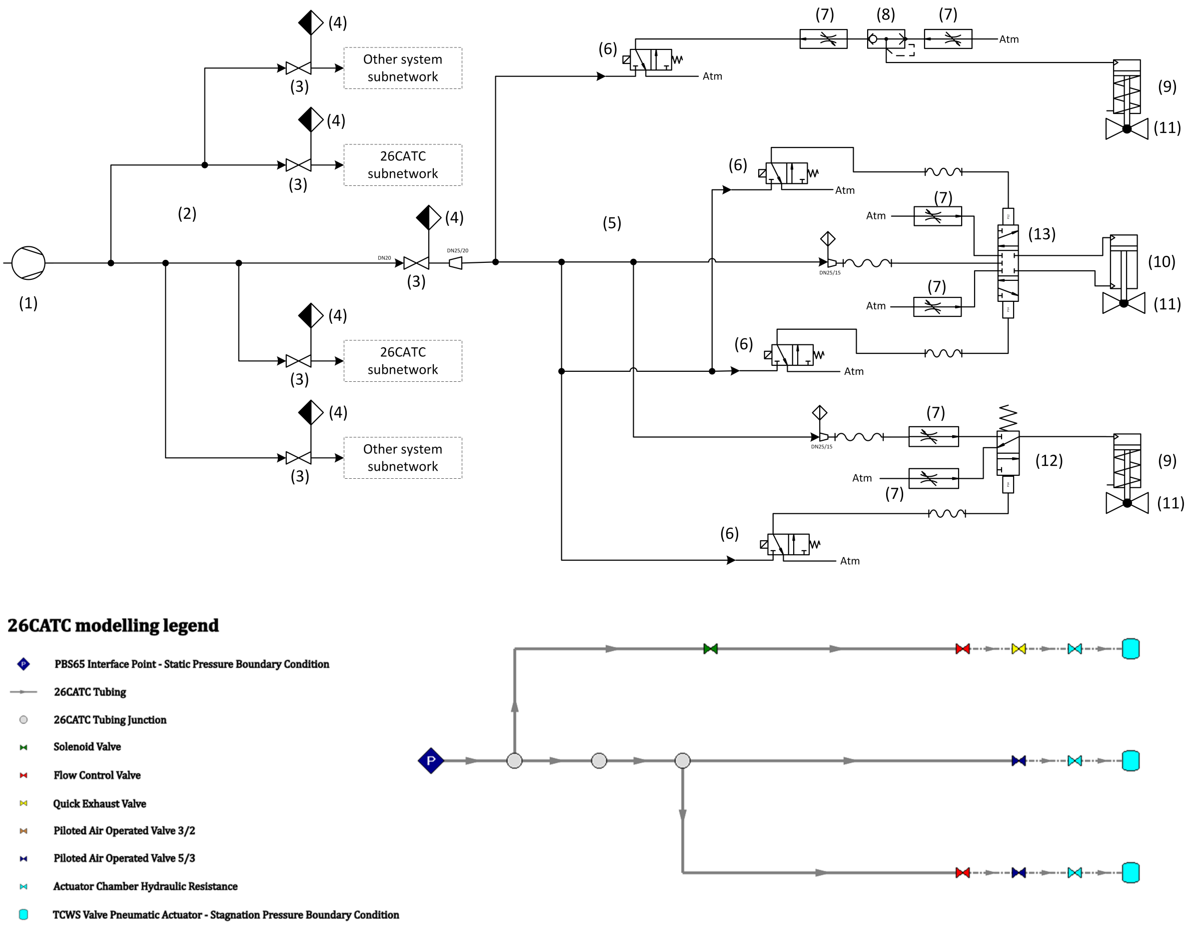

Figure 6.4: Example: Arrow model snippet (bottom) of the 26CATC schematic (top). The Arrow model only includes the tubes leading to the actuator chamber itself, pilot ports are neglected. (1) Compressor Station, (2) Compressed Air Distribution System, (3) gate valve, (4) Interface Point, (5) 26CATC, (6) Solenoid Valve, (7) Flow Control Valve, (8) Quick Exhaust Valve, (9) Single-Acting Pneumatic Actuator, (10) Double-Acting Pneumatic Actuator, (11) TCWS Valve, (12) 3/2 AOV, (13) 5/3 AOV

Further down, the models include every junction, with a color code applied to make identification easier in large systems. The actuator chamber inlet resistances are modelled with a separate valve symbol to add further precision to the models. The last few model valves (the Flow Control Valve, and occasionally the Quick Exhaust Valve) are connected by zero-length connectors, as these are mounted directly onto the actuators and the connecting hoses pose negligible hydraulic resistances. The models end at the downstream stagnation pressure boundaries (tanks), chosen because the actuator chambers are similar to small pressure vessels. An example of the built Arrow models is shown in Figure 6.5.

After building the Arrow model shells, the next step was to add hydraulic resistance data to obtain more

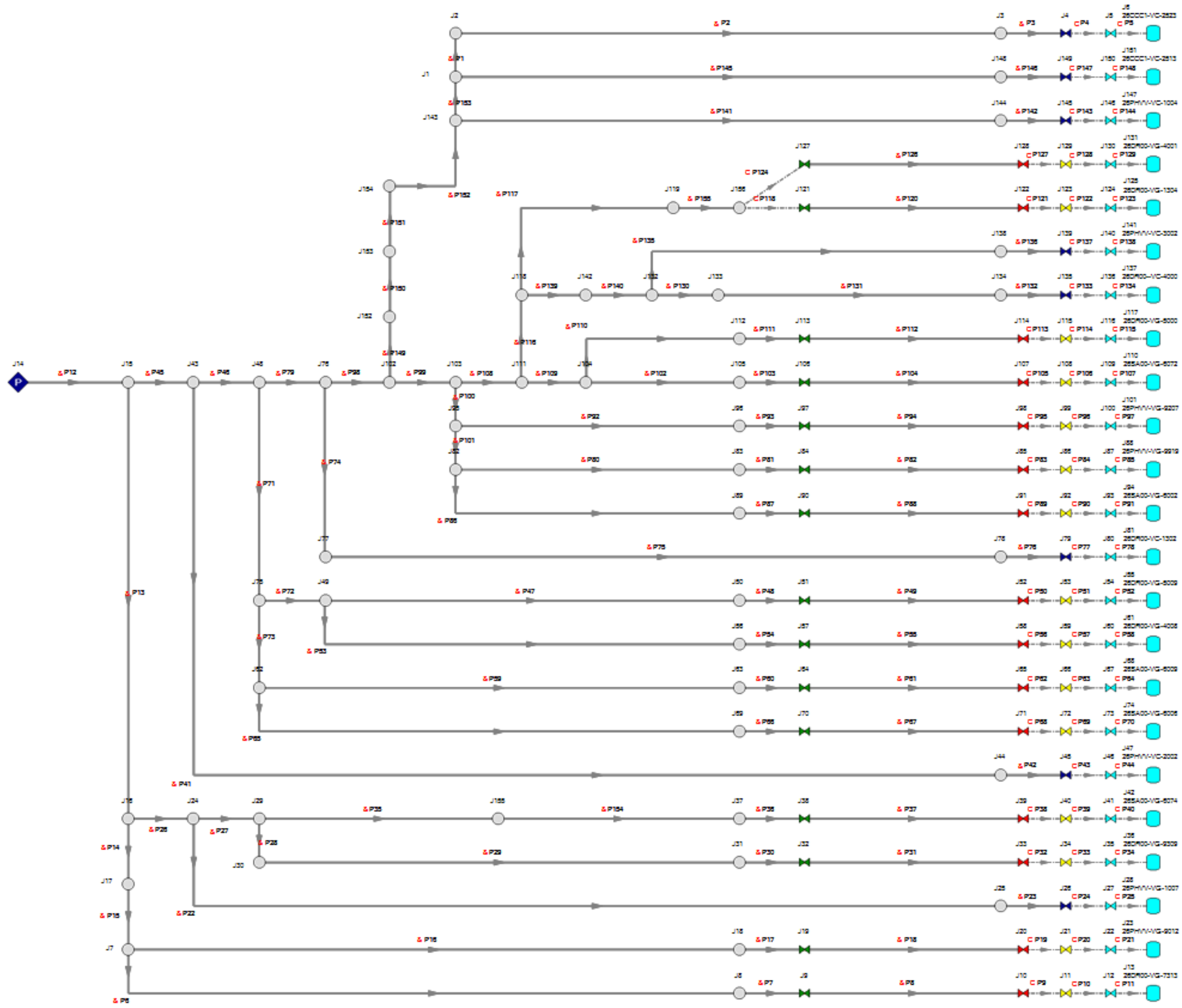

Figure 6.5: Example: Interface point 6511CA-VG-0511 - Arrow model. The model is used to account for the worst case scenario for stroking times. It considers the minimum declared pressure upstream, and conservative pressures enough to safely open the actuators as described in Section 6.1.1. The models further include the resistance of the 26CATC network, and the valves required for commanding the TCWS valves along the way (Section 6.1.2. The model is further used to create TCWS safety and operational scenarios, to be discussed in 6.1.3. For the figure legend, see Figure 6.4

accurate mass flow rate values during valve opening. This step not only improved the precision of the network representation but also established a method that simplifies future updates and verifications of the models.

In the 26CATC system, some interface points are located more than 50 meters from their actuators. The narrow and crowded installation spaces in between lead to long, winding piping routes. Manually entering every bend, reducer, expander, tee, and wye would have required months of repetitive work. To address this challenge, ITER already had two useful resources: a 3D model of the proposed layout and an Excel macro capable of calculating and exporting hydraulic resistances from pre-organized isometric data into AFT Arrow.

However, several steps still required careful preparation. The raw data from the 3D model first had to be filtered and organized, since each resistance element was exported as an individual entry. To create a structured table suitable as macro input, the resistances had to be grouped by their corresponding pipes, component types, sizes, and unique features such as bend angles, expander and reducer dimensions, and tee properties. This was achieved by writing several additional VBA codes. Next, the original ITER macro itself was updated and divided into smaller modules to allow for intermediate checks and debugging. Finally, the processed isometric data were imported into the appropriate Arrow model at the pipe level.

This workflow was used to build 61 Arrow models, incorporating more than 6,000 pipe entries and organizing over 100,000 resistance records. The entire process was automated through VBA scripts. Although constructing all models required substantial effort, the detailed procedural description is not directly relevant to the reader and is therefore omitted.

Modelling hydraulic resistances means the Arrow models now contain a high-quality physical representation of the proposed layout, providing accurate simulation results and a solid foundation for future nuclear safety calculations. Moreover, the data transformation method developed from the 3D CAD model into AFT Arrow makes future updates simple and straightforward. The written macros serve as a tool for data organization, resistance calculation, and Arrow import. Since it allows the user to repeat all actions with just a few clicks, it will be used by ITER for several more years in case of future design changes.

6.1.3. Operating scenarios

With the model scope and boundary conditions defined, and the Arrow models built and filled with pipe isometrics and resistance data, the only missing part is the simultaneous operation of valves. In TCWS, certain scenarios require multiple valves to operate at once, either as part of Safety Functions or other operations per system.

Safety Functions are the valve actions required when an accident occurs at ITER, a standard feature in both conventional and experimental reactors. For example, in the event of a LOCA (Loss of Coolant Accident), ITER specifies several valves that must open or close within the required time. Depending on the actuator type and the command, some actuators will need compressed air to move. A Fail-in-Position valve, for instance, may need to fully open or fully close, while Fail-Open and Fail-Close valves are designed to reach their safe state without compressed air.

The number of valves involved in a Safety Function can vary widely, and this has a direct impact on the network. When several actuators draw air at the same time, the flow through shared pipes increases. This raises the pressure drop in those segments, which in turn reduces the available Δp for downstream actuators. The result is a lower mass flow rate and longer stroke times. For this reason, stroke time compliance must also be checked under these "worst-case" simultaneous operation scenarios.

Another important aspect is the simultaneous operation of valves per system. At the start of a plasma cycle, valves are opened at the same time. Furthermore, during plasma operation, the simultaneous control of valves from the same system is a likely scenario. It is important to verify the valve stroking times for non safety-important valves with this limiting case as well.

To conclude, the scenarios implemented into each AFT Arrow model are:

- Safety Functions
- Valve operation per system

A worked example of the valve selection for scenarios is given in Table 6.2 for interface point 6511CA-VG-0511. The 23 valves at this location are involved in two Safety Functions that require compressed air. Of these five, only two include an FP valve, both requiring 26PHVV-VG-1007. Furthermore, there are four TCWS systems being operated from this interface point. These are CCC1 (Component Cooling), DR00 (Draining), SA00 (Sampling), PHVV (Primary Heat Transfer - Vacuum Vessel Cooling).

Table 6.2: Mass flow rate results from AFT Arrow for pressurisation scenarios from the supply side for interface point 6511CA-VG-0511. The used scenarios are N-009 (Safety Function for Vacuum Vessel - Decay Heat Removal), N-011 (Safety Function for Vacuum Vessel - Loss of Coolant Accident), CCC1 (Component Cooling), DR00 (Draining), SA00 (Sampling), PHVV (Primary Heat Transfer - Vacuum Vessel Cooling).

Valve tag	Safe Failure	Stroke Time Verification Scenarios					
		Safety Functions		System Operation			
		N-009	N-011	CCC1	DR00	SA00	PHVV
26CCC1-VC-2513	FP			✓			
26CCC1-VC-2523	FP			✓			
26DR00-VC-1302	FP				✓		
26DR00-VG-1304	FC				✓		
26DR00-VC-4000	FP				✓		
26DR00-VG-4001	FC				✓		
26DR00-VG-4008	FC				✓		
26DR00-VG-5000	FC				✓		
26DR00-VG-5009	FC				✓		

Continued on next page

Valve tag	Safe Failure	Stroke Time Verification Scenarios (continued)					
		Safety Functions		System Operation			
		N-009	N-011	CCC1	DR00	SA00	PHVV
26DR00-VG-7313	FC				✓		
26DR00-VG-9309	FC				✓		
26PHVV-VC-1004	FP						✓
26PHVV-VC-2002	FP						✓
26PHVV-VC-3002	FP						✓
26PHVV-VG-1007	FP	✓	✓				
26PHVV-VG-9012	FC						✓
26PHVV-VG-9207	FC						✓
26PHVV-VG-9919	FC						✓
26SA00-VG-6002	FC					✓	
26SA00-VG-6006	FC					✓	
26SA00-VG-6009	FC					✓	
26SA00-VG-6072	FC					✓	
26SA00-VG-6074	FC					✓	

6.1.4. Stroke Time Calculation

With the Arrow models fully prepared and the scenarios defined, the final step is to run the simulations. Since the pipes are relatively short and heat transfer effects are negligible, adiabatic flow is assumed. All compressed air valves are considered fully open, and their hydraulic resistances have been pre-defined in the AFT Arrow libraries from the available datasheets.

The software starts by solving the fundamental continuity and momentum equations for every pipe element, as well as the continuity and energy equations for every branch. Since the boundary conditions given are all pressure type, the code starts by iterating on the mass flow rate and modifying the intermediate pressure values until a unique solution is found. Arrow employs a modified Newton–Raphson matrix method to achieve a system-level balance of mass, energy, and concentration. Upon completion of the solving process, the continuity and energy equations are satisfied at all branching points within the network. After convergence, Arrow performs a verification step in which it iterates through each junction, summing the inflows and outflows of mass and energy, and comparing these totals against predefined solution tolerances. If any junction is found to deviate beyond the acceptable limits, the software issues a corresponding warning in the output. A more thorough description of compressible flow equations in pipes, through valves, and their usage in the Arrow simulations applied to the present task can be found in Appendix B. [26]

Once the calculation converged, the software automatically exports to a corresponding Microsoft Excel file equipped with a VBA macro that organizes and structures the generated data. Subsequently, another VBA script collects and consolidates the exported results. For each valve, the relevant minimum flow rate is selected. This function is necessary in case there are several Safety Functions associated with the same valve. It is used to select the ”worst-case” flow rate, i.e. when several other valves are triggered at the same time. The study uses this flow value as the flow rate entering the actuator at any given moment after the pilot and solenoid delay.

Based on the actuator model, command type, and fail-safe configuration, the same datasheet computes the pressurization stroking times according to Equation 6.2. Since the used flow rate exported from Arrow is calculated with a conservative minimal pressure drop estimation along the line, calculating both pressurisation (*Latent*) times and stem movement (*Active*) times gives a similarly conservative estimation of the stroking times.

$$t_{\text{stroke}} = \frac{V_{\text{chamber}} \cdot \rho(p_{\text{BC}})}{\dot{m}} + \frac{V_{\text{dead}} \cdot \rho(p_{\text{BC}})}{\dot{m}} + \frac{V_{\text{tubing}} \cdot \rho(p_{\text{BC}})}{\dot{m}} + t_{\text{pilot}} \tag{6.2}$$

where the parameters are defined as follows:

- $\rho(p_{\text{BC}})$ – the density of air at the AFT Arrow boundary condition pressure.
- V_{chamber} – the volume of the pressurised chamber. For Fail in Position valves, the larger chamber volume is considered. This is the only fill-up making up the *Active* phase (T_{3b}).
- V_{dead} – the dead volume of the specific actuator. For rack-and-pinion actuators, this is approximately 25% of the total chamber volume, while there is no dead volume for linear types [25]. Filling up the dead volume is included in the *Latent* phase (T_{3a}).

- V_{tubing} – the tubing volume from the solenoid valve to the actuator. This delay is only applicable for Direct Control valves. This is conservatively estimated as 50 m of 3/8" Schedule 20 piping (2.4 L) [25]. Filling up the tubing is included in the *Latent* phase (T_{3a}).
- $\dot{m}$ – the AFT Arrow mass flow rate. The selected flow rate is the minimum given flow rate by the "worst-case" scenario - i.e. when the overall network consumption is the highest.
- t_{pilot} – the time delay of the solenoid valve and the time to pressurise the pilot ports. This is pre-calculated and is used as a constant per command type [25]:
  - 0.5 s for Direct Control
  - 1.2 s for Piloted Air Operated Valve (Fail Open / Fail Close)
  - 1.3 s for Piloted Air Operated Valve (Fail in Position)

For the depressurization process of Fail Open and Fail Close actuators, as well as for the opposite chamber in Fail in Position actuators, the actuator supplier is responsible for conducting experimental tests and verifying the corresponding stroke times.

6.2. Consumption Calculation

Sizing the Compressed Air Network for the Tokamak Cooling Water System (TCWS) involves three key steps. So far, the focus has been on stroke time verification—a necessary but not sufficient part of the design. Once stroke times are confirmed to be below the maximum allowable values, the next step is to evaluate whether the compressor station can supply the required amount of air. This evaluation is carried out in the present Consumption Calculation. To complete the sizing process, the final step will address network protection, including the selection, sizing, and placement of Pressure Reducing Valves (PRVs).

The Consumption Calculation assesses the air demand in two ways: peak and continuous consumption of TCWS valves. For practical reasons, both values are calculated per interface point. Peak demand occurs when multiple valves request compressed air simultaneously, either during normal operation or during a triggered Safety Function (see Section 6.1.3). Peak consumption is mainly determined by two factors: (i) the peak demand of a single TCWS valve, and (ii) the number of valves operating at the same time. Continuous demand, by contrast, represents the amount of compressed air required by valves during regular operation. The key factor here is the number of valves that need a constant air supply to perform their function.

Peak Consumption

The peak consumption of a single valve is defined as the mass flow rate required to meet the average stroking time. As discussed earlier, stroking time defines the minimum and maximum times needed for a valve to open or close. In the Stroke Time Verification calculation, the valves were verified to operate within the required maximum time. Minimum times are handled differently: each valve layout includes a Flow Control Valve (FCV) to throttle the flow, thereby increasing the stroking time. During commissioning, the FCVs will be adjusted under process conditions to ensure the stroking times fall within the specified range. If stroke times exceed the maximum even with the FCVs fully open, design modifications are necessary.

Peak consumption depends on two factors: (i) the peak demand of a single TCWS valve, and (ii) the number of valves operating simultaneously. As noted in Section 6.1.1, the physics inside the pneumatic actuator chamber are delicate, with chamber pressure often varying during stem movement. Examining instantaneous valve demand would be tedious and inappropriate for the current design maturity. A practical approach is to assess the peak demand over the entire *Active* phase of the stroke. This is justified for two reasons: first, T_{3a} (the *Latent* phase) is short compared to the full stroke, so it does not represent the overall demand; second, the load data for the *Active* phase allows identification of a chamber pressure sufficient to move the highest load. Using this pressure, the total air mass required to fill the chamber can be estimated with the ideal gas law.

Using this pressure, the total air mass required to fill the chamber can be estimated using the ideal gas law. The peak demand is defined per valve by defining a mass flow rate:

$$\dot{m} = \frac{V \cdot \rho(5 \text{ bar(g)})}{t} \tag{6.3}$$

where $\rho(5 \text{ bar(g)})$ is the density of air at 5 barg pressure. This pressure is a conservative estimation of the required pressure to open the valve during maximum sizing process loading conditions (see more in Section 6.1).

$$\rho(5 \text{ bar(g)}) = 7.13 \text{ kg/m}^3 \tag{6.4}$$

The total pressurised volume V for each combination of actuator and command type is defined as:

$$V = V_{\text{chamber}} + V_{\text{dead}} + V_{\text{tubing}} \tag{6.5}$$

- V_{chamber} – the volume of the pressurised chamber. For FP valves, the larger chamber volume is considered.
- V_{dead} – the dead volume of the specific actuator. For rack-and-pinion actuators, this is approximately 25% of the total chamber volume, while there is no dead volume for linear types [25]. Filling up the dead volume is included in the *Latent* phase (T_{3a}).
- V_{tubing} – the tubing volume from the solenoid valve to the actuator. Only applicable for DC valves. This is conservatively estimated as 50 m of 3/8” Schedule 20 piping (2.4 L) [25].

Here, t is the average required stroking time, reduced by the time delay of the solenoid and the AOV pilot ports:

$$t = \frac{t_{\text{stroke,min}} + t_{\text{stroke,max}}}{2} - t_{\text{pilot}} \tag{6.6}$$

- $t_{\text{stroke,min}}$ and $t_{\text{stroke,max}}$ – the defined required stroking times of each valve for pressurisation cases: FO – closing, FC – opening. For FP valves, the smaller stroke time is considered.
- t_{pilot} – the time delay of the solenoid valve and the time to pressurise the pilot ports. This has been calculated before and is used as a constant per command type [25]:
  – 0.5 s for DC
  – 1.2 s for Piloted AOV FO/FC
  – 1.3 s for Piloted AOV FP

After calculating the peak demand for each valve, the next step is to determine which valves operate concurrently. This process is similar to the method described in the Stroke Time Verification Calculation. Firstly, Safety Functions require multiple valves to pressurise simultaneously. Only Fail-in-Position valves are considered, since FO and FC valves are designed to perform their safety function without air supply. The further scenarios considered are: the operation of valves belonging to the same system, the valves operating during Plasma Operation, and all control valves of the specific interface point.

A key difference from the Arrow Scenarios is the last two cases: peak demand for valves operating during Plasma Operation, and all control valves of the interface point. The reason for this is that both contain mainly control valves throttling the flow by small air pulses entering the chambers during the whole operation. Stroking times in these cases are not important, however, the cumulated valve peak consumption can be excessive.

An overview of the defined scenarios is presented in Table 6.3 for interface point 6511CA-VG-0511. The table shows each valve connected to the specific interface point selected for the above mentioned scenarios. Six scenarios have been defined based on ITER Safety Functions and system operation. The Safety Functions include N-009 (Safety Function for Vacuum Vessel - Decay Heat Removal) and N-011 (Safety Function for Vacuum Vessel - Loss of Coolant Accident). Both of these require compressed air supply in case of a trigger. They only concern a single valve, 26PHVV-VG-1007. For TCWS operation, the concerned systems are CCC1 (Component Cooling), DR00 (Draining), SA00 (Sampling), PHVV (Primary Heat Transfer - Vacuum Vessel Cooling). Alongside system operation, the two additional scenarios defined were the valves operating during Plasma Operation and all control valves.

Table 6.3: Valve peak consumption calculation selection for interface point 6511-VG-0511. The used scenarios are N-009 (Safety Function for Vacuum Vessel - Decay Heat Removal), N-011 (Safety Function for Vacuum Vessel - Loss of Coolant Accident), CCC1 (Component Cooling), DR00 (Draining), SA00 (Sampling), PHVV (Primary Heat Transfer - Vacuum Vessel Cooling), Control Valve Operation, and Operation During Plasma Operation of ITER.

Valve tag	Peak Consumption Calculation Selection							
	Safety Functions		System Operation				Control Valve Operation	Operation During Plasma
	N-009	N-011	CCC1	DR00	PHVV	SA00		
26CCC1-VC-2513			✓				✓	✓
26CCC1-VC-2523			✓				✓	✓
26DR00-VC-1302				✓			✓	
26DR00-VG-1304				✓				
26DR00-VC-4000				✓			✓	
26DR00-VG-4001				✓				
26DR00-VG-4008				✓				
26DR00-VG-5000				✓				
26DR00-VG-5009				✓				
26DR00-VG-7313				✓				
26DR00-VG-9309				✓				
26PHVV-VC-1004					✓		✓	✓
26PHVV-VC-2002					✓		✓	
26PHVV-VC-3002					✓		✓	
26PHVV-VG-1007	✓	✓			✓			✓
26PHVV-VG-9012					✓			
26PHVV-VG-9207					✓			
26PHVV-VG-9919					✓			
26SA00-VG-6002						✓		

Continued on next page

Valve tag	Peak Consumption Calculation Selection (continued)							
	Safety Functions		System Operation				Control Valve Operation	Operation During Plasma
	N-009	N-011	CCC1	DR00	PHVV	SA00		
26SA00-VG-6006						✓		
26SA00-VG-6009						✓		
26SA00-VG-6072						✓		
26SA00-VG-6074						✓		

For each scenario i, the individual peak demands for each valve k are summed up per interface point j:

$$\dot{m}_{\mathrm{i,j}} = \sum_{k=0}^{n} \dot{m}_{i,j,k} \tag{6.7}$$

To determine whether the Compressed Air Distribution System can supply this demand, an acceptance criterion must be defined for each interface point. This is provided by the presizing document [32], which specifies a preferred maximum value of $52 \frac{\mathrm{Nm}^3}{\mathrm{h}}$.

Continuous Consumption

After determining the peak consumption for each interface point, the continuous consumption must be assessed. Continuous demand is a key sizing input for the compressor station and represents the main cost driver for the system. As discussed earlier, continuous consumption is driven by valves that require a steady air supply to perform their function. Most of these are control functions managing flow, pressure, and temperature within the TCWS, and many are Fail-in-Position types, needing compressed air to move in both directions. Their consumption during a single cycle can be estimated using chamber pressures and volumes as previously described.

The main question is how long do these valves control the flow. As a general guideline, four full back-and-forth cycles per valve and 20 minutes of full operation per hour for TCWS control valves has been assumed [33]. This assumption is justified by the relatively small temperature dead-band in the cooling lines and the significant fluctuations in cooling power caused by plasma pulsing and disruption events, which require continuous flow adjustments during Plasma Operation.

Valve selection for continuous consumption follows the same method as for peak consumption. However, Safety Functions are not considered, as they are rarely triggered, and per-system operation is generally executed only at the start of Plasma Operation. To get a good representation of it, the first scenario selects the control valves open during Plasma Operation, and then calculates the number of total cycles (back-and-forth) it would take to operate continuously for 20 minutes straight. It then adds four additional full cycles, and calculates the total consumed volume of air in $\frac{\mathrm{Nm}^3}{\mathrm{h}}$ (Eq. 6.8). This is the total compressed air consumption for each control valve every hour. The calculation repeats this for another scenario, where all control valves are considered to operate simultaneously. This is an extreme scenario without any physical background, but is still a useful insight for maximum demand sizing.

$$\dot{m} = \left(4 + \frac{1200}{t}\right) \cdot V_{\mathrm{avg}} \tag{6.8}$$

where t is the average of the average required stroking times for closing and opening:

$$t = \frac{\frac{t_{\mathrm{open,min}} + t_{\mathrm{open,max}}}{2} + \frac{t_{\mathrm{close,min}} + t_{\mathrm{close,max}}}{2}}{2} \tag{6.9}$$

which gives an average time considering both opening and closing stroke time requirements. Eq. 6.8 gives the average volume of the actuators' chambers by considering equal operation in both directions:

$$V_{\mathrm{avg}} = \frac{V_{\mathrm{ch,in}} + V_{\mathrm{ch,out}}}{2} \tag{6.10}$$

where:

- $V_{\mathrm{ch,in}}$ – the volume of the center chamber.
- $V_{\mathrm{ch,out}}$ – the volume of the outside chamber.

The applied valve selection for the two scenarios is shown for interface point 6511CA-VG-0511 in Table 6.4:

Table 6.4: Continuous consumption calculation valve selection of interface point 6511CA-VG-0511. The used scenarios are (i) control valves operaing during Plasma Operation, and (ii) all control valves.

Valve tag	**Continuous Consumption Calculation Selection**	
	Control Valve During PO	**All Control Valves**
26CCC1-VC-2513	✓	✓
26CCC1-VC-2523	✓	✓
26DR00-VC-1302		✓
26DR00-VG-1304		
26DR00-VC-4000		✓
26DR00-VG-4001		
26DR00-VG-4008		
26DR00-VG-5000		
26DR00-VG-5009		
26DR00-VG-7313		
26DR00-VG-9309		
26PHVV-VC-1004	✓	✓
26PHVV-VC-2002		✓
26PHVV-VC-3002		✓
26PHVV-VG-1007		
26PHVV-VG-9012		
26PHVV-VG-9207		
26PHVV-VG-9919		
26SA00-VG-6002		
26SA00-VG-6006		
26SA00-VG-6009		
26SA00-VG-6072		
26SA00-VG-6074		

With the selection criteria ready, a VBA macro calculates the selected air flow rates for each interface point. The preferred acceptance criteria from the Liquid and Gas Distribution System is 10 $\frac{\mathrm{Nm}^3}{\mathrm{h}}$ [29].

6.3. Pressure Reducing Valve Sizing

After stroke times were verified in Section 6.1, the previous section provided an overview of the peak and continuous consumption calculations and assessed whether the compressor station can supply the required compressed air. This central compressed air network serves as the source for all distributed air across ITER, so the supply pressure must meet the demands of various systems throughout the plant. This results in a declared static pressure range of 7 barg to 11 barg at the interface point (see Figure 6.2 and Section 6.1).

This range establishes the upstream boundary and model boundary condition for the Stroke Time Verification calculation. However, it also presents a challenge: many downstream components in the 26CATC network—such as certain actuators, solenoid valves, and Quick Exhaust Valves—cannot handle the full 11 barg supply pressure. A color-scaled figure highlights these vulnerable components in Figure 6.6. On the figure, the red color represents a maximum allowable pressure of 7 barg, while the completely blue parts mark a maximum allowable pressure more than 11 barg. The components' respective pressure limits are summarized in Table 6.5.

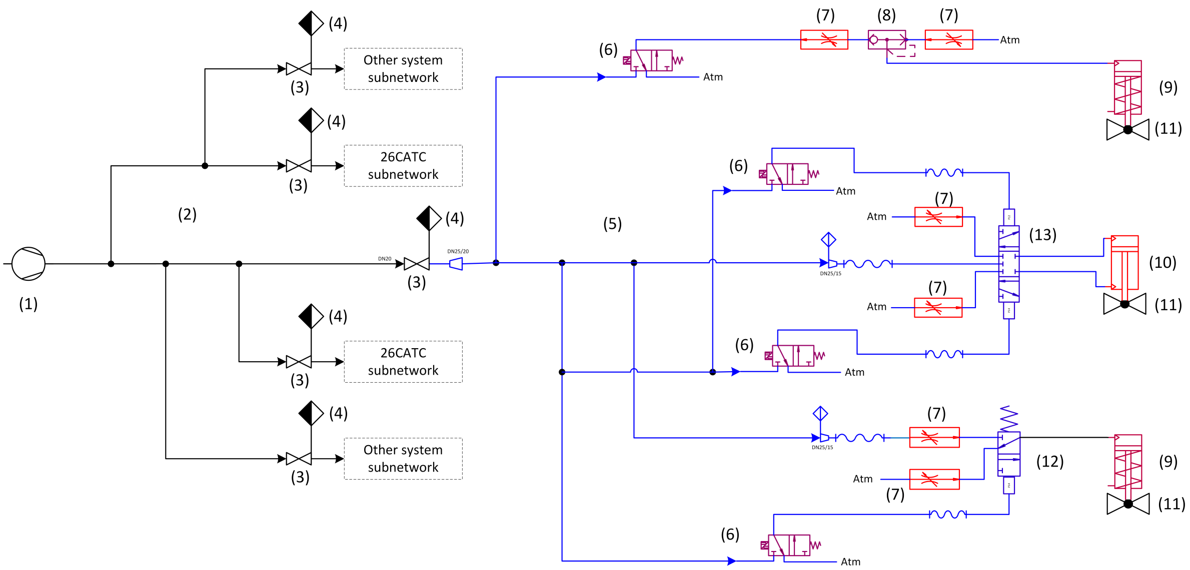

Figure 6.6: Schematic diagram of 26CATC network colored by protection need. Red - maximum allowable pressure is 7 barg, Blue - maximum allowable pressure more than 11 barg

Table 6.5: Maximum Allowable Pressures of the 26CATC Network Parts

Nr.	Network Part Name	p_{max}, barg
(5)	Tubing, Flexible Hoses and Junctions	≥ 11
(6)	Solenoid Valve	8.6
(7)	Flow Control valve	N/A
(8)	Quick Exhaust Valve	8.6
(9)	Single-Acting Pneumatic Actuator	8
(10)	Double-Acting Pneumatic Actuator	$7 - 9.5$ based on type
(12)	3/2 Air operated Valve	10.3
(13)	5/3 Air operated Valve	10.3

Table 6.5 shows that most network components have a maximum allowable pressure below the highest pressure at the 26CATC interface. In fact, some linear pneumatic actuators cannot exceed 7 barg, the lowest declared interface pressure. This indicates that nearly all network parts require pressure protection, some more critically than others. In industrial practice, such situations are managed using Pressure Reducing Valves (PRVs), which regulate downstream pressure consistently.

PRVs are designed to maintain a set downstream pressure regardless of upstream fluctuations. Their main role is to ensure safe and reliable operation by protecting pipelines, equipment, and end-users from excessive pressure. The working principle relies on balancing a spring force against the hydraulic force of the controlled fluid. Figure 6.7 shows a PRV's schematic drawing [34].When the downstream pressure rises above the setpoint—adjusted by tightening the spring (8)—the increase is sensed via the internal pressure port (6). The diaphragm (7) is pushed up, moving the main valve (5) via the valve stem (3) closer to the valve seat (4). This increases the pressure drop and reduces downstream pressure. Conversely, if the downstream pressure falls below the setpoint, the spring (8) pushes the diaphragm (7) downward, opening the main valve (5) fully and raising the downstream pressure.

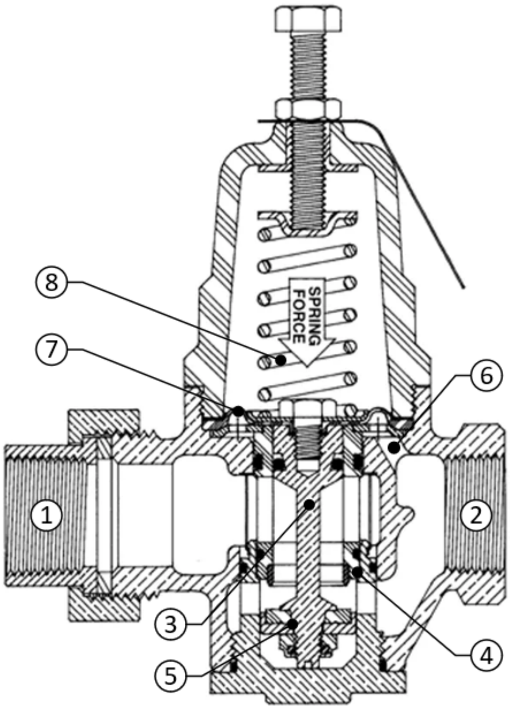

Figure 6.7: Pressure Reducing Valve drawing [34], modified by the author. (1): Inlet port, (2) Outlet port, (3) Valve stem, (4) Valve seat, (5) Main valve, (6) Pressure Sensing Port, (7) Diaphragm, (8) Spring

The design and selection of an appropriate PRV into the 26CATC depends on three main factors: flow rate, operating pressure range, and location. In the present system, flow rate is governed by the valve operation discussed in Section 6.2, the pressure limit of vulnerable network parts (Table 6.5) and the declared interface point pressures. The PRV location is determined by the scope of protection required.

Estimating the mass flow rate is critical to selecting the correct PRV size. As illustrated in Figure 6.7, the fluid passes through a complex geometry that introduces a significant pressure drop. If the valve is undersized, the flow can become choked, causing an excessive pressure drop downstream and potentially invalidating all previous calculations. Figure 6.8 shows an example PRV performance curve. For a correctly sized valve, the flow remains controllable across the full operating range and the pressure drop is minimal. For undersized valves, higher flow rates result in excessive pressure drops as the valve chokes, which is unacceptable for the 26CATC network during operation. Choked flow reduces the mass flow rate, leading to an increase in stroking times.

To avoid choking the network, it is essential to know the estimated flow rate through the PRV's proposed place. This information has already been calculated in Section 6.2, where the consumption for each valve and interface point was summarized for the main "worst-case" scenarios. These values can therefore be used directly as input for the sizing.

The second main factor in sizing is the location. This is closely tied to the desired network pressures. The interface point will have pressures between 7 barg to 11 barg, while downstream network components have various maximum allowable pressures according to their catalogues. An obvious approach is to protect the network from the start: placing a PRV immediately after the gate valve and setting it to 7 barg would shield the entire network from overpressure, as shown in Figure 6.9. However, this approach would prevent certain non safety-important valves from opening under maximum process loading conditions.

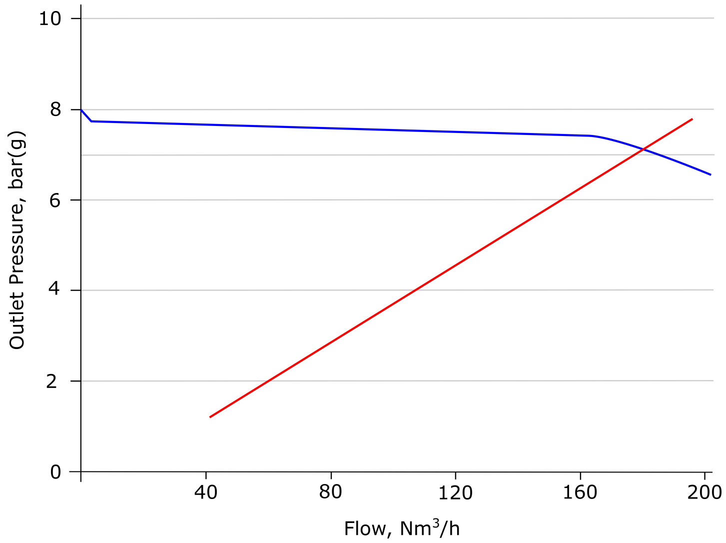

Figure 6.8: Pressure Reducing Valve curve, with an inlet pressure of 9 barg, and a pressure setting of 7.8 barg. The blue curve represents the outlet pressure of the valve at different flow rates, while the red curve shows the 30 $\frac{m}{s}$ flow velocity at different outlet pressures [35].

The issue of opening NON-SIC valves was highlighted in Section 6.1.1 when torque curves were examined to define simulation boundary conditions. It was concluded that if the supply pressure does not reach the required 7 barg at the start of opening, the valves might fail to operate under maximum process loads. If the PRV at the interface point produces a significant pressure drop, the actuators could fail to open. To address this, it is recommended to increase the PRV pressure setting at the interface point. This is feasible since the next most sensitive components are Single-Acting Pneumatic Actuators with a maximum pressure tolerance of 8 barg. Consequently, PRVs on the main line can be set to 8 barg at zero flow, protecting most of the network while minimally affecting flow.

The remaining unprotected components are the few Double-Acting actuators with low pressure tolerance (7 barg). To individually protect each actuator before the Piloted AOV (mounted directly on the actuator body), additional PRVs can be installed right before the Flow Control Valve. This is illustrated in the middle command line for an FP valve in Figure 6.9. For each valve, the opening pressure requirement has been checked to ensure the PRVs do not prevent operation. Using this approach, each interface point has a main PRV immediately after the gate valve and a few additional PRVs to protect sensitive Double-Acting actuators directly at their locations.

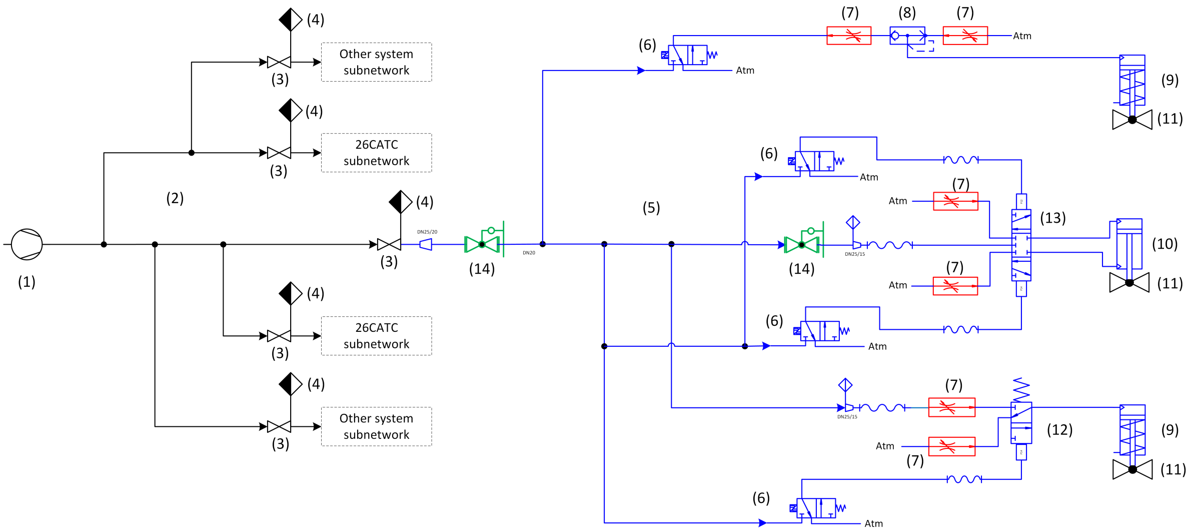

Figure 6.9: Schematic of the ITER Compressed Air Network with the proposed location of the Pressure Reducing Valves (14)

On the other hand, adding one more valve can significantly increase the hydraulic resistance of the specific line, potentially lengthening stroke times for the corresponding valve. Therefore, re-verification of the stroke times is required by modelling the PRV resistance in AFT Arrow. This creates an iterative loop for every interface point: sizing the PRV, checking stroke times, and resizing the PRVs if the maximum allowable stroking time is exceeded.

An important caveat arises when a NON-SIC valve requires 7 barg to open, but the interface point pressure is also 7 barg at that moment. In this case, the pressure downstream will not be sufficient to open the valve, regardless of PRV settings. The only solution is to request an increase of the supply pressure from the Compressed Air Distribution System engineers, which has been done at the time of writing this study.

Finally, it is necessary to assess whether the PRVs introduce any safety concerns. The critical scenario is a fire in the rooms housing the TCWS valves and the 26CATC system. In a fire, the uninsulated network can experience rapid temperature spikes, heating the compressed air inside the pipes. With no space to expand, trapped air could cause a dangerous overpressure, risking damage to the network. Examining the PRV behavior, one finds that if a fire downstream increases the downstream pressure, the PRV will close as designed. This would trap air between the PRV locations and downstream solenoid or air-operated valves. To mitigate this risk, a bypass valve configuration is proposed, as shown in Figure 6.10. This arrangement allows higher-pressure air to escape upstream and vent safely through Pressure Relief Valves installed either upstream of the interface point or on the upper ports of closed solenoid valves.

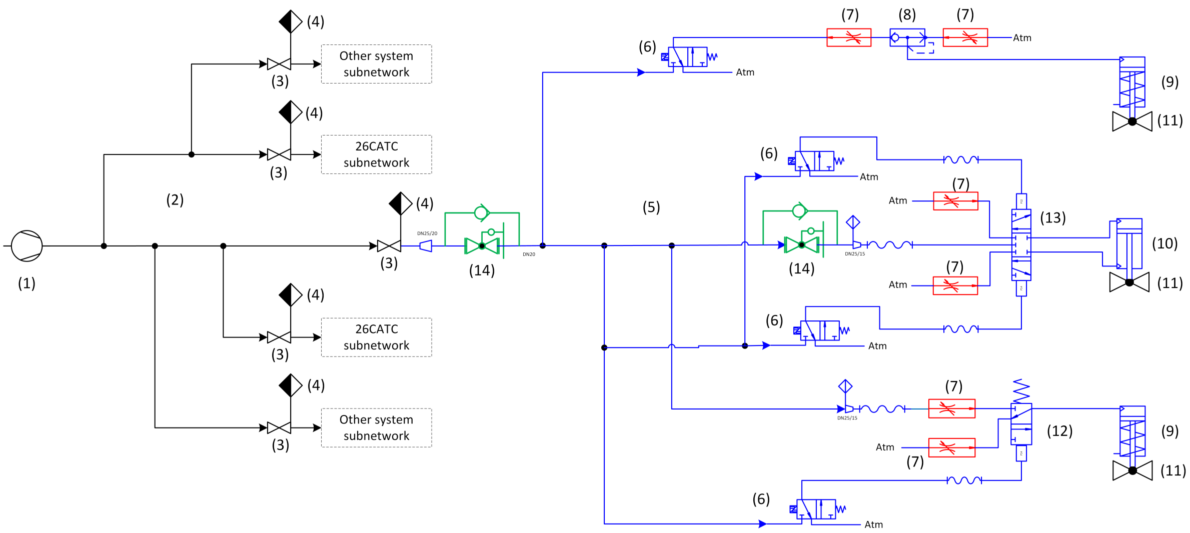

Figure 6.10: Schematic of the ITER Compressed Air Network with the proposed location and final design of the Pressure Reducing Valves (14), including the bypass valve

With this, the PRV sizing is concluded. By selecting the appropriate flow rate, pressure setting, and location, and by designing the auxiliary bypass valve in parallel, the PRV ensures overpressure protection for all downstream network components.

7
Results

7.1. Stroke Time Verification Calculation

The Stroke Time Verification Calculation assesses the achievable stroking times for all Tokamak Cooling Water System (TCWS) actuated valves by modelling the hydraulic resistances of ITER's Compressed Air System for Tokamak Cooling (26CATC). Each actuated valve is connected to a 26CATC subnetwork, which, in turn, is connected to the ITER Liquid and Air Distribution Network. Each subnetwork is modelled with a single AFT Arrow file, and all connected actuators' stroking times are calculated based on the model results. In total, 61 Arrow models have been created for a total of 1012 actuated valves. For each Arrow model, operational scenarios were created to model the ITER TCWS's operation, including Safety Functions and subsystem demand. Given the upstream and downstream pressure boundary conditions, the software iterates to calculate the forming mass flow rate for each actuator. This is then automatically exported to a corresponding Microsoft Excel file equipped with a VBA macro organising information. The results are then automatically collected and organized by another VBA code from the 26CATC System Sizing Datasheet. The same datasheet then calculates the pressurisation stroking times based on the actuator model, the command type, and the fail-safe mode of the specific valve, following the method discussed in Section 6.1. For the de-pressurisation of Fail Open and Fail Close actuators, and the de-pressurisation of the opposite chamber for Fail in Position actuators, the actuator supplier has to conduct tests and verify the associated stroke times.

An example of the forming mass flow rates for the defined scenarios at interface point 6511CA-VG-0511 is presented in Table 7.1. There are 23 valves connected to this interface point; the associated Arrow model is shown in Figure 6.5. The models include all tubing losses extracted, organised and calculated from the available 3D models, and also include all 26CATC valve losses associated with the command types of each valve. The boundary conditions represent the pressure at which each specific valve is able to open. Six scenarios have been defined based on ITER Safety Functions and system operation. The Safety Functions include N-009 (Safety Function for Vacuum Vessel - Decay Heat Removal) and N-011 (Safety Function for Vacuum Vessel - Loss of Coolant Accident). Both of these require compressed air supply in case of a trigger. They only concern a single valve, 26PHVV-VG-1007. Since the primary function of this valve is executing the associated Safety Function, it is not considered in any other subsequent scenario regarding operational purposes. For TCWS operation, the concerned systems are CCC1 (Component Cooling), DR00 (Draining), SA00 (Sampling), PHVV (Primary Heat Transfer - Vacuum Vessel Cooling). Each valve uses a valve tag in which the four letters after the Plant Breakdown System (for CWS, this is 26) denote the respective system. The associated valves are selected to require compressed air during the Arrow simulation, achieving a realistically lower flow rate as a result compared to modelling just a single line. The resulting flow rates are displayed in $\frac{\mathrm{kg}}{\mathrm{h}}$, while the last column selects the minimum flow rate value for each valve in order to minimise the stroking times. This last function is necessary in case there are several Safety Functions associated with the same valve. It is used to select the "worst-case" flow rate, i.e. when several other valves are triggered at the same time.

Table 7.1: Mass flow rate results from AFT Arrow for pressurisation scenarios from the supply side for interface point 6511CA-VG-0511. The used scenarios are N-009 (Safety Function for Vacuum Vessel - Decay Heat Removal), N-011 (Safety Function for Vacuum Vessel - Loss of Coolant Accident), CCC1 (Component Cooling), DR00 (Draining), SA00 (Sampling), PHVV (Primary Heat Transfer - Vacuum Vessel Cooling).

Valve tag	**Safe failure**	**Mass flow rate during pressurisation, $\frac{kg}{h}$**						**Minimum flow rate, $\frac{kg}{h}$**
		N-009	**N-011**	**CCC1**	**DR00**	**SA00**	**PHVV**	
26CCC1-VC-2513	FP			60.5				60.5
26CCC1-VC-2523	FP			61.6				61.6
26DR00-VC-1302	FP				66.3			66.3
26DR00-VG-1304	FC				10.0			10.0
26DR00-VC-4000	FP				34.8			34.8
26DR00-VG-4001	FC				10.0			10.0
26DR00-VG-4008	FC				10.5			10.5
26DR00-VG-5000	FC				12.1			12.1
26DR00-VG-5009	FC				10.4			10.4
26DR00-VG-7313	FC				12.8			12.8
26DR00-VG-9309	FC				13.1			13.1
26PHVV-VC-1004	FP						52.9	52.9
26PHVV-VC-2002	FP						43.6	43.6
26PHVV-VC-3002	FP						59.9	59.9
26PHVV-VG-1007	FP	103.2	103.2					103.2
26PHVV-VG-9012	FC						11.8	11.8
26PHVV-VG-9207	FC						11.3	11.3
26PHVV-VG-9919	FC						11.0	11.0
26SA00-VG-6002	FC					16.5		16.5
26SA00-VG-6006	FC					16.4		16.4
26SA00-VG-6009	FC					16.4		16.4
26SA00-VG-6072	FC					25.6		25.6
26SA00-VG-6074	FC					26.0		26.0

After collecting the mass flow rates from the Arrow simulations, stroke times are calculated using Equation 6.2. These results are then compared against the required limits to verify compliance. In order to carry out these calculations on all 1012 actuated valves, a VBA code base has been created. The code samples actuator data, command type, and fail-safe position to establish the used volumes, as well as the valve tag to identify the pressurisation mass flow rate in case of a relevant scenario.

Table 7.2: Stroke Time Verification Calculation results for interface point 6511CA-VG-0511. The mass flow rate results have been exported from AFT Arrow, while the Arrow boundary condition is based on the available torque or force curves. The stroking times have been calculated with Equation 6.2. All valves have been verified to comply with stroke time requirements for this interface point.

Valve tag	**Safe fail-ure**	**Maximum allowable stroking time,** s	**Arrow mass flow rate,** $\frac{kg}{h}$	**Arrow boundary condition,** barg	T_{3a}, s	T_{3b}, s	T_3, s	**Verified?**
26CCC1-VC-2513	FP	30	60.5	5.0	2.64	5.38	8.02	YES
26CCC1-VC-2523	FP	30	61.6	5.0	2.62	5.28	7.90	YES
26DR00-VC-1302	FP	30	66.3	5.0	1.30	0.52	1.82	YES
26DR00-VG-1304	FC	30	10.0	5.3	7.34	5.49	12.84	YES
26DR00-VC-4000	FP	60	34.8	5.0	1.58	1.11	2.68	YES
26DR00-VG-4001	FC	30	10.0	5.3	7.34	5.49	12.82	YES

Continued on next page

Valve tag	**Safe fail-ure**	**Maximum allowable stroking time,** s	**Arrow mass flow rate,** $\frac{\mathrm{kg}}{\mathrm{h}}$	**Arrow boundary condition,** barg	T_{3a}, s	T_{3b}, s	T_3, s	**Verified?**
26DR00-VG-4008	FC	30	10.5	5.3	6.97	5.20	12.17	YES
26DR00-VG-5000	FC	30	12.1	5.0	6.13	5.55	11.68	YES
26DR00-VG-5009	FC	30	10.4	5.3	7.05	5.26	12.31	YES
26DR00-VG-7313	FC	60	12.8	5.0	7.01	9.96	16.97	YES
26DR00-VG-9309	FC	30	13.1	5.0	5.71	5.14	10.85	YES
26PHVV-VC-1004	FP	30	52.9	5.0	3.46	8.66	12.12	YES
26PHVV-VC-2002	FP	30	43.6	5.0	3.16	7.45	10.62	YES
26PHVV-VC-3002	FP	30	59.9	5.0	1.30	0.17	1.47	YES
26PHVV-VG-1007	FP	50	103.2	5.0	5.65	17.42	23.07	YES
26PHVV-VG-9012	FC	30	11.8	5.0	7.53	10.74	18.27	YES
26PHVV-VG-9207	FC	30	11.3	5.0	6.20	4.58	10.78	YES
26PHVV-VG-9919	FC	30	11.0	5.0	8.06	11.55	19.61	YES
26SA00-VG-6002	FC	30	16.5	5.0	3.78	0.66	4.44	YES
26SA00-VG-6006	FC	30	16.4	5.0	3.81	0.67	4.47	YES
26SA00-VG-6009	FC	30	16.4	5.0	3.81	0.67	4.47	YES
26SA00-VG-6072	FC	30	25.6	5.0	2.62	0.43	3.04	YES
26SA00-VG-6074	FC	30	26.0	5.0	2.58	0.42	3.00	YES

As an example, the stroking times of two valves are considered here. 26DR00-VG-1304 is a Fail Close DN50 ball valve without safety classification, operated by a single-acting (spring assist) pneumatic actuator. Since the valve is Fail Close, it closes by using its springs in case of losing the compressed air supply. In order to open the valve, the actuator's center chamber must be pressurised. The available time to open is $30\,\mathrm{s}$ according to the stroke time requirements. Based on the available valve calculation notes and torque curves, it has been previously established that the valve must open at $5.3\,\mathrm{barg}$ during maximal process loading conditions. The valve is most likely to be operated together with other valves belonging to the DR00 (Draining) system. The mass flow rate calculated by AFT Arrow for the Draining system operation scenario is $10.0\,\frac{\mathrm{kg}}{\mathrm{h}}$. From the ideal gas law, the air density at the required pressure ($5.3\,\mathrm{barg}$) is $7.49\,\frac{\mathrm{kg}}{\mathrm{m}^3}$. The actuator is commanded via the Direct Control configuration, using a solenoid valve to allow air flow into the actuator. It has been previously established that the solenoid delay is $0.5\,\mathrm{s}$ for this command mode, and that the tubing volume from the solenoid valve to the actuator is $2.4\,\mathrm{L}$. The actuator's center chamber has a volume of $2.41\,\mathrm{L}$, and a dead volume of $25\,\%$ of the chamber volume ($0.60\,\mathrm{L}$). In the *Latent phase* (T_{3a}), three sources of delay are considered. The solenoid delay comes from the solenoid valve's response time to the electric signal, this is $0.5\,\mathrm{s}$. Moreover, the tubing from the solenoid valve to the actuator chamber, as well as the actuator chamber dead volume, needs to be pressurised to the opening pressure. The combined time for this with the AFT Arrow flow rate is $8.63\,\mathrm{s}$. It is important to note that the flow rate is highly conservative, since in the beginning of pressurisation, the available pressure drop between the interface point and the actuator chamber is significantly higher than the boundary conditions AFT Arrow is working with. For the *Active Phase*, the chamber volume is filled up at the boundary condition pressure. This takes $6.53\,\mathrm{s}$, making up a total time of $15.16\,\mathrm{s}$. Since the calculated value is below the required stroke time ($30\,\mathrm{s}$), the valve passes the verification.

The second valve is 26PHVV-VG-1007, a DN450 Fail in Position butterfly valve with the primary function of isolation in case of Loss of Coolant Accident. It is operated in case of two Safety Functions: N-009 - Safety Function for Vacuum Vessel Decay Heat Removal, and N-011 - Safety Function for Vacuum Vessel Loss of Coolant Accident. It is operated by a double-acting pneumatic actuator, requesting compressed air for operation in every case. In order to open the valve, the actuator's center chamber must be pressurised, while for closing, the outside chamber is supplied. The available time for both actions is $50\,\mathrm{s}$ according to the stroke time requirements. Based on the available valve calculation notes and torque curves, it has been previously established that the valve must open at $5\,\mathrm{barg}$ during maximal process loading conditions. The mass flow rate calculated by AFT Arrow for the Safety Function scenarios is $103.2\,\frac{\mathrm{kg}}{\mathrm{h}}$. From the ideal gas law, the air density at the required pressure ($5\,\mathrm{barg}$) is $7.13\,\frac{\mathrm{kg}}{\mathrm{m}^3}$. The actuator is commanded via a 5/3 Piloted Air Operated Valve, where the solenoid and pilot port pressurisation delay is estimated to be $1.3\,\mathrm{s}$. To remain conservative, the calculation uses the larger actuator chamber volume, which is in this case the outside chamber ($84\,\mathrm{L}$). The actuator also has a dead volume which corresponds to $25\,\%$ of the outside chamber volume (21 L). In the *Latent phase* (T_{3a}), the solenoid and pilot port delay, and the dead volume pressurisation takes $6.52\,\mathrm{s}$, while the *Active Phase* is estimated to take $20.90\,\mathrm{s}$, making up a total time of $27.42\,\mathrm{s}$. Since the calculated value is below the required stroke time ($50\,\mathrm{s}$), this valve also passes the verification.

In total, the calculation found 108 valves that do not comply with the stroke time requirements. 87 of them are Fail in Position valves with no safety classification, and Fail Close valves where pressurisation is not associated with the valves' safety function. These are generally PHBD valves connected to interface points on Level 3 of the Tokamak Building. This level contains 542 PHBD valves, therefore the assumption to operate the system at the same time is a significant overestimation of the actual future demand of the network. Hence the current report suggests sequential valve operation for these interfaces.

The calculation also found that 21 Fail in Position valves have a Safety Function where they are not able to respect their stroking time requirements. All of them are located in the same room and have a primary function to carry out the IBED - LOCA 2 (Integrated Blanket, ELM, and Divertor - Loss of Coolant Accident) Safety Function. This function can be triggered by a pipe break on the IBED TCWS cooling loop, and these 21 valves are responsible to isolate the lines in order to prevent contaminated water escaping or flooding the Tokamak Building. At the moment, these valves use the biggest available actuator and due to their extreme process loading conditions, they require compressed air to close. However, the current design considers their supply from just two interface points. This means that when the IBED - LOCA 2 function is triggered, the network will not be able to supply the valves in the required time.

To tackle this challenge, several solutions have been proposed. One of them is the spring-assist configuration of the current Fail in Position valve. This means that two springs would be included into the actuator to help closing the valve. However, this would increase the torque required to open, which could not be supplied by the present network conditions. Another possibility is to increase the pipe size leading to the actuators from DN20 to DN80. Although this looks to be an easy solution, the compressor station already in place is not able to supply such a demand, and the piping layout in the already congested Tokamak Building would need to be significantly modified. The third solution is designing a pneumatic accumulator next to the valves. This accumulator would provide the air supply in case the Safety Function is triggered, while other regular valve activities such as flow control, would remain supplied by the 26CATC network already in place. Although this solution is most likely to prevail, in case of a fire event, the pressure vessel becomes a source of danger. The current report therefore recommends the implementation of an additional pressure vessel next to these valves, with additional fire protection measures such as insulation and Pressure Relief Valves.

Lastly, valve 26PHVV-VG-1107 complies with its required stroking time, but with only $18\,\%$ safety margin. Its calculated closing time is ($42.3\,\mathrm{s}$), while the requested value is ($50\,\mathrm{s}$). Interface point 6511CA-VG-1511 supplies compressed air to the actuator. Although this does not seem to be a possible issue, it takes away the possibility of stroke time control with the Flow Control Valve, and does not leave margin for considering degraded environmental conditions. The valve is also required to operate by two Safety Functions, the already mentioned VV-LOCA and VV-DHR ones. It is therefore important to find a solution resulting in lower stroking times.

For this valve, the limiting scenario was found to be the VV-DHR function, which commands five more Fail in Position valves to obtain a different position in case of a triggering event. This limits the available flow rate for 26PHVV-VG-1107 and since it has a large actuator, the stroking time exceeds the maximum limit. To tackle the problem, the present report suggests connecting the valve to a different compressed air interface point inside the same room - 6511CA-VG-1512. These valves are all located in room 11-L2-01 of the Tokamak Building, which also hosts 6511CA-VG-1512 - an interface point identical in both Safety Classification and the used safety train to the currently used one. It does not currently have any valves requesting compressed air in case of the VV-DHR or the VV-LOCA Safety Functions, making it a perfect candidate for the task.

7.2. Consumption Calculation

Once stroke times have been verified, the network's compressed air consumption is assessed. The method first calculates the individual consumption of each valve per cycle, based on the average stroking time. This time is achieved by throttling the flow using the Flow Control Valve. Next, the valves are selected based on the defined scenarios. These include Safety Functions, system operation, valves operating during Plasma Operation, and Control Valve Operation. For each interface point, all valves requesting compressed air in a relevant scenario are collected, and their individual consumptions are summed. Table 7.3 presents the used method for interface point 6511CA-VG-0511. The individual peak consumptions are listed next to each valve on the interface, and the selected valves for each scenario are marked. The communicated consumption threshold for each interface point $52\,\frac{\mathrm{Nm}^3}{\mathrm{h}}$ [29].

Continuous consumption is assessed for control valves only. These are all Fail in Position valves, which throttle the flow using the the pressurisation of both actuator chambers. The calculation assumes four full back-and-forth strokes and 20 minutes of temperature control every hour for each valve. The resulting continuous consumption is assessed for two scenarios: control valves operating during plasma operation, and for all control valves. The valve selection for each scenario is marked in Table 7.3. The communicated maximum allowable continuous consumption threshold is $10\,\frac{\mathrm{Nm}^3}{\mathrm{h}}$ [29].

For all interface points, the assessment was carried out using an Excel calculation, with a macro automating the steps described above. The results are summarised in the last row of Table 7.3. Two Safety Functions require compressed air, both triggering valve 26PHVV-VG-1007 to close in the event of an incident. The peak demand for this valve is $62.7\,\frac{\mathrm{Nm}^3}{\mathrm{h}}$, already over the criteria threshold. When evaluating the other demands, the calculation finds that the peak demand per system is $124.1\,\frac{\mathrm{Nm}^3}{\mathrm{h}}$, $117.7\,\frac{\mathrm{Nm}^3}{\mathrm{h}}$ during Plasma Operation, and $73.9\,\frac{\mathrm{Nm}^3}{\mathrm{h}}$ for control valves. All three exceed the threshold.

Looking at the continuous consumption, the results also indicate a significant excess demand. The control valves operating during Plasma Operation request around $13.5\,\frac{\mathrm{Nm}^3}{\mathrm{h}}$, while when considering all control valves, one could expect a $18.3\,\frac{\mathrm{Nm}^3}{\mathrm{h}}$ average flow. Both of these exceed the pre-determined threshold.

The results indicate that the current design at this interface point is insufficient to meet all peak demands based on the criteria given by the Liquid and Gas Distribution System. However, this does not mean the demand cannot be physically met. It is nevertheless clear that the two engineering teams need to work on a solution deviating from the current criteria. As this will be part of a future assessment, any further calculations exceed the scope of this thesis.

Table 7.3: Valve peak and continuous consumption calculation selection. Valve peak consumption calculated using an average stroking time.

Valve tag	**Valve peak consumption,** $\mathrm{Nm^3/h}$	**Peak Consumption Calculation Selection**								**Continuous Consumption Calculation Selection**	
		Safety Functions		**System Operation**				**Control Valve Operation**	**Operation During Plasma**	**Control Valve During PO**	**All Control Valves**
		N-009	**N-011**	**CCC1**	**DR00**	**PHVV**	**SA00**				
26CCC1-VC-2513	16.14			✓				✓	✓	✓	✓
26CCC1-VC-2523	16.14			✓				✓	✓	✓	✓
26DR00-VC-1302	1.23				✓			✓			✓
26DR00-VG-1304	7.51				✓						
26DR00-VC-4000	1.10				✓			✓			✓
26DR00-VG-4001	7.51				✓						
26DR00-VG-4008	7.51				✓						
26DR00-VG-5000	4.71				✓						
26DR00-VG-5009	7.51				✓						
26DR00-VG-7313	4.71				✓						
26DR00-VG-9309	4.71				✓						
26PHVV-VC-1004	22.72					✓		✓	✓	✓	✓
26PHVV-VC-2002	16.14					✓		✓			✓
26PHVV-VC-3002	0.41					✓		✓			✓
26PHVV-VG-1007	62.71	✓	✓			✓			✓		
26PHVV-VG-9012	7.32					✓					
26PHVV-VG-9207	7.51					✓					
26PHVV-VG-9919	7.32					✓					
26SA00-VG-6002	4.22						✓				
26SA00-VG-6006	4.22						✓				
26SA00-VG-6009	4.22						✓				
26SA00-VG-6072	4.22						✓				
26SA00-VG-6074	4.22						✓				
Total		**62.71**	**62.71**	**32.27**	**46.52**	**124.13**	**21.08**	**73.86**	**117.69**	**13.46**	**18.31**

The results per interface point for all interfaces located in Room 11-B2-01 (Drain Tank Room) of the Tokamak Building are summarised in Table 7.4. Only the highest consumption value of each scenario is displayed. The total analysis consisted of conducting the above calculation for 61 interface points. The total number of evaluated consumption calculation valve selections was 2112.

When looking at all interface points, the study finds that safety concerns arise at only five locations. A safety concern is defined here as a case where the requested air flow rate exceeds the $52\,\frac{\mathrm{Nm^3}}{\mathrm{h}}$ peak consumption threshold during the execution of a Safety Function. Additionally, 35 out of the 66 interface points may experience demands exceeding the mentioned limit during their life, which represents a significant concern for future operation.

When continuous demand is considered, values range from 0 to $68.5\,\frac{\mathrm{Nm^3}}{\mathrm{h}}$, with 10 out of 66 interface points requesting more than $10\,\frac{\mathrm{Nm^3}}{\mathrm{h}}$. This raises questions about the cumulative demand across the entire 26CATC system and whether the compressor station will be able to supply the required air.

Table 7.4: Peak and continuous consumption calculation results for each relevant peak and continuous consumption scenario. The table shows a total of 8 interface points located in Room 11-B2-01 (Drain Tank Room) of the Tokamak Building. The total number of interface points is 61.

Interface Point	**Peak Demand Calculations, $\frac{\mathrm{Nm^3}}{\mathrm{h}}$**				**Continuous Demand Calculations, $\frac{\mathrm{Nm^3}}{\mathrm{h}}$**	
	Safety Functions	**Per System**	**During PO**	**Control Valves**	**Control Valves Open During PO**	**All Control Valves**
6511CA-VG-0511	62.7	124.1	117.7	73.9	13.5	18.3
6511CA-VG-1511	71.0	76.4	77.0	6.5	1.0	1.9
6511CA-VG-0127	0.0	5.8	0.0	1.2	0.0	0.5
6511CA-VG-0510	0.0	87.9	0.0	1.2	0.0	0.5
6511CA-VG-0459	3.0	21.1	0.0	0.0	0.0	0.0
6511CA-VG-0509	0.0	89.2	89.2	90.4	20.8	21.2
6511CA-VG-0512	0.0	31.4	4.7	0.0	0.0	0.0
6511CA-VG-1512	0.0	63.7	4.7	0.0	0.0	0.0

In conclusion, the results indicate that several interface points are undersized, and for most, the $52\,\frac{\mathrm{Nm^3}}{\mathrm{h}}$ limit is likely to be exceeded during the system's operational lifetime. Five interface points show that the threshold is surpassed when a Safety Function is triggered, implying that additional measures will be necessary. Furthermore, interface point 6511CA-VG-1285 demonstrates a particular vulnerability, as Safety Function N-010 (IBED-LOCA-2, Integrated Blanket, ELM and Divertor – Loss of Coolant Accident) requests more than $1000\,\frac{\mathrm{Nm^3}}{\mathrm{h}}$ of compressed air. The proposed suggestions for this interface have already been presented in Section 7.1.

7.3. Pressure Reducing Valve Sizing

Previously, the consumption calculation demonstrated that current demands exceed the upstream network's limits. Nevertheless, these calculated demands must be met, meaning that Pressure Reducing Valve (PRV) sizing must be carefully performed, taking into account potential design modifications and their impact on the system. In any case, the network command modes and fittings remain unchanged, so the PRV requirements will persist in the future.

The need for overpressure protection of the whole 26CATC network has been identified beforehand in Chapter 4. This was due to the maximum possible interface point pressure of 11 barg, and the maximum allowable pressure of almost all network valves, together with all pneumatic actuators. Section 6.3 proposed a solution, which protects the network in two distinct places: one PRV right after the interface point set to 8 barg, and one PRV for each vulnerable actuator with a maximum allowable pressure of 7 barg. The reducers are set to 7 barg when protecting the individual actuators.

The sizing of the PRVs considered three limiting factors: the PRV must maintain its control function at the sizing flow rate, the pressure outlet of the PRV cannot be more than 1 bar lower than the pressure setting at the sizing flow rate, and the flow velocity must remain below 30 $\frac{\mathrm{m}}{\mathrm{s}}$ on the downstream side to maintain control stability. The sizing flow rate is the peak flow given by the Consumption Calculation at the specific PRV location. The complete sizing process was automated through an Excel macro by manually creating a library from the selected manufacturer's catalogues where all relevant sizing data was displayed. Then, the code collects the sizing flow rates and all necessary PRV locations, and selects the smallest PRV fulfilling the above mentioned requirements.

As an example, interface point 6511CA-VG-0511 is considered. Here, four PRVs are needed to protect the network from overpressure: one main-line PRV right after the interface point, and three protecting valves with vulnerable actuators: 26PHVV-VG-1007, 26PHVV-VC-3002, and 26DR00-VC-1302. The sizing flow rates can be found in Table 7.4 for the interface point, and Table 7.3 for the three valves equipped with vulnerable actuators. If more consumption scenarios are listed for a single interface point, the maximum demand flow rate is selected as the sizing value. For the first PRV, the limiting scenario is the PHVV system operation (124.1 $\frac{\mathrm{Nm}^3}{\mathrm{h}}$), while for the other valves, it is the protected actuators' individual peak consumptions. Using this information and the manually created PRV library, the macro selected two a DN15 and a DN20 PRV. Their specifications are presented in Table 7.5.

Table 7.5: Pressure Reducing Valves selected for interface point 6511CA-VG-0511. The relevant curves for the PRVs are shown: 1 - Figure 7.1, 2 - Figure 7.2, 3,4 - Figure 7.3

PRV Number	PRV Requirement				Selected PRV			
	Location	**Sizing flow rate,** $\frac{\mathrm{Nm}^3}{\mathrm{h}}$	**Sizing inlet pressure range,** barg	**Outlet pressure require-ment,** barg	**Size**	**Control range,** barg	**Pressure Setting,** barg	C_V
1	Interface point	124.1	7–11	≤ 8	DN20	0–68.9	7.8	2.3
2	Before actuator	1.2	0–8	≤ 7	DN15	1.7–17.2	6.8	1.95
3	Before actuator	0.4	0–8	≤ 7	DN15	1.7–17.2	6.8	1.95
4	Before actuator	62.7	0–8	≤ 7	DN20	0–68.9	6.8	2.3

PRV 1 is required immediately downstream of the interface point. The sizing mass flow rate is 124.1 $\frac{\mathrm{Nm}^3}{\mathrm{h}}$, while the upstream pressure can vary between 7 barg to 11 barg. The required outlet pressure is a maximum of 8 barg. Based on this, a DN20 PRV has been selected with its curve shown in Figure 7.1. The blue line represents the PRV control curve at 9 barg inlet pressure. For very small flow rates, one finds a sharp drop in pressure because it is difficult for the regulator to maintain pressure at this location. This is called the seat load drop, and due to it, the pressure setting of the PRV is decreased to 7.8 barg. As the curve continues for higher flow rates, the droop remains fairly constant throughout the entire range, with the choked flow region not depicted

by the present curve. One the other hand, the red line shows the flow rate achievable at the maximum line speed suggested by the manufacturer (30 $\frac{\mathrm{m}}{\mathrm{s}}$). This is the maximum downstream velocity at which the regulator can safely maintain its control function. Based on the above mentioned constraints, the maximum allowable mass flow rate for this PRV and pressure setting is $180\,\frac{\mathrm{Nm}^3}{\mathrm{h}}$, safely above the sizing flow rate.

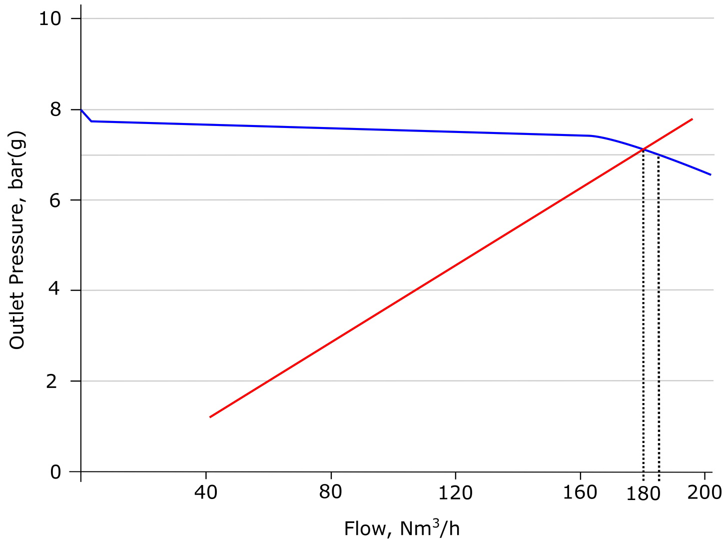

Figure 7.1: Curves of *PRV 1* with an inlet pressure of $9\,\mathrm{barg}$, and a pressure setting of $7.8\,\mathrm{barg}$. The blue curve represents the outlet pressure of the valve at different flow rates, while the red curve shows the 30 $\frac{\mathrm{m}}{\mathrm{s}}$ flow velocity at different outlet pressures. The maximum allowable flow through the valve is limited by the flow velocity constraint, resulting in a flow rate of $180\,\frac{\mathrm{Nm}^3}{\mathrm{h}}$.

PRV 2 regulates the flow upstream of the actuator for valve 26PHVV-VG-1007. The sizing mass flow rate corresponds to the peak demand of this actuator: $62.7\,\frac{\mathrm{Nm}^3}{\mathrm{h}}$. As it is further downstream, it is protected by *PRV 1*, giving it an operating range of $0\,\mathrm{barg}$ to $8\,\mathrm{barg}$. The required outlet pressure is a maximum of $7\,\mathrm{barg}$. After careful consideration, the same DN20 PRV valve is proposed, with its curve shown in Figure 7.2. The reader can note tha for a lower pressure setpoint, the curve is shifted down, and the maximum allowable flow rate through the valve is reduced to $145\,\frac{\mathrm{Nm}^3}{\mathrm{h}}$. The pressure setting is $6.8\,\mathrm{barg}$ in order to avoid excessive pressures at very low flow rates.

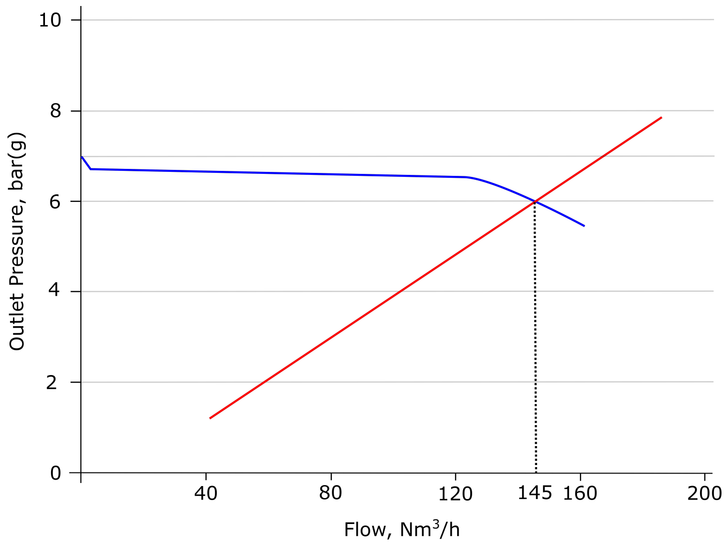

Figure 7.2: Curves of *PRV 1* with an inlet pressure of $8\,\mathrm{barg}$, and a pressure setting of $6.8\,\mathrm{barg}$. The blue curve represents the outlet pressure of the valve at different flow rates, while the red curve shows the 30 $\frac{\mathrm{m}}{\mathrm{s}}$ flow velocity at different outlet pressures. The maximum allowable flow through the valve is limited by the flow velocity constraint, resulting in a flow rate of $145\,\frac{\mathrm{Nm}^3}{\mathrm{h}}$.

For valves 26PHVV-VC-3002, and 26DR00-VC-1302, the DN20 PRV is too large. With their low individual peak consumption, the smallest process regulator has been chosen from the manufacturer series. The reducer's curve is shown in Figure 7.3, displaying the maximum allowable flow of 60 $\frac{\mathrm{Nm}^3}{\mathrm{h}}$. This is still a significant oversizing, but the current cost and qualification limits, as well as available catalogues have made the selected PRV the best candidate.

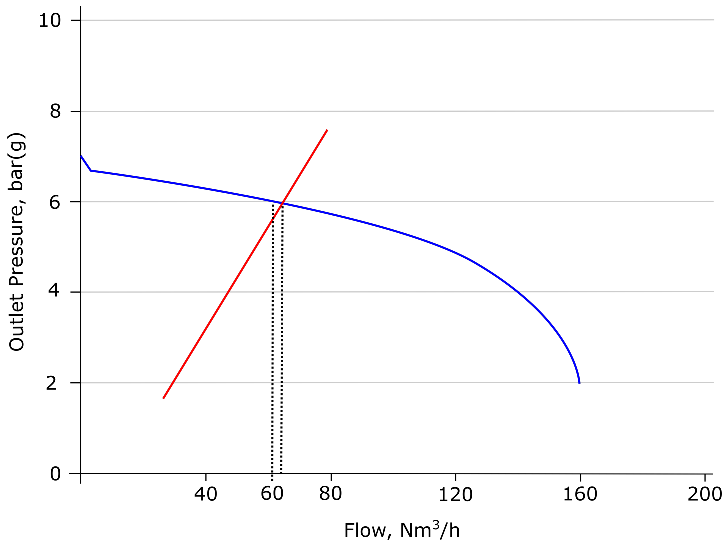

Figure 7.3: Curves of *PRV 2* with an inlet pressure of 8 barg, and a pressure setting of 6.8 barg. The blue curve represents the outlet pressure of the valve at different flow rates, while the red curve shows the 30 $\frac{\mathrm{m}}{\mathrm{s}}$ flow velocity at different outlet pressures. The maximum allowable flow through the valve is limited by the 1 bar pressure drop constraint, resulting in a flow rate of 60 $\frac{\mathrm{Nm}^3}{\mathrm{h}}$.

With this, interface point 6511CA-VG-0511 is fully sized. The same approach has been followed for the remaining 60 interfaces, with a total of 168 valves sized. Table 7.6 shows the selected PRVs for interface points inside Room 11-B2-01 (Drain Tank Room) of the Tokamak Building. The table covers a total of 8 interfaces out of 61. The sizing used three different PRVs to optimize qualification and cost considerations.

Table 7.6: Pressure Reducing Valves selected for interface points inside Room 11-B2-01 (Drain Tank Room) of the Tokamak Building. The table covers a total of 8 interfaces out of 61. All PRVs maintain a control range containing the sizing inlet pressure range.

PRV Requirement					**Selected PRV**		
Interface point	**Location**	**Sizing flow rate,** $\frac{\mathrm{Nm}^3}{\mathrm{h}}$	**Sizing inlet pressure range,** barg	**Outlet pressure requirement,** barg	**Size**	**Maximum allowable flow rate,** $\frac{\mathrm{Nm}^3}{\mathrm{h}}$	**Pressure Setting,** barg
6511CA-VG-0511	Interface point	124.1	7–11	≤ 8	DN20	180	7.8
6511CA-VG-0511	Before actuator	1.23	0–8	≤ 7	DN15	60	6.8
6511CA-VG-0511	Before actuator	0.4	0–8	≤ 7	DN15	60	6.8
6511CA-VG-0511	Before actuator	62.7	0–8	≤ 7	DN20	145	6.8
6511CA-VG-1511	Interface point	77.0	7–11	≤ 8	DN20	180	7.8
6511CA-VG-1511	Before actuator	1.4	0–8	≤ 7	DN15	60	6.8
6511CA-VG-1511	Before actuator	1.4	0–8	≤ 7	DN15	60	6.8
6511CA-VG-1511	Before actuator	62.7	0–8	≤ 7	DN20	145	6.8
6511CA-VG-0127	Interface point	5.8	7–11	≤ 8	DN15	70	7.8
6511CA-VG-0127	Before actuator	1.2	0–8	≤ 7	DN15	145	6.8
6511CA-VG-0510	Interface point	87.9	7–11	≤ 8	DN20	180	7.8

Continued on next page

PRV Requirement					Selected PRV		
Interface point	**Location**	**Sizing flow rate,** $\frac{Nm^3}{h}$	**Sizing inlet pressure range,** barg	**Outlet pressure requirement,** barg	**Size**	**Maximum allowable flow rate,** $\frac{Nm^3}{h}$	**Pressure Setting,** barg
6511CA-VG-0510	Before actuator	1.2	0–8	≤ 7	DN15	60	6.8
6511CA-VG-0459	Interface point	21.1	7–11	≤ 8	DN15	60	7.8
6511CA-VG-0509	Interface point	90.4	7–11	≤ 8	DN20	180	7.8
6511CA-VG-0512	Interface point	31.4	7–11	≤ 8	DN15	60	7.8
6511CA-VG-1512	Interface point	63.7	7–11	≤ 8	DN15	145	7.8

8

Conclusion and future work

This study aims to design the ITER's Compressed Air System for Tokamak Cooling (26CATC). The system is operating the project's primary cooling loop, the Tokamak Cooling Water System (TCWS). The design focused on three main goals, namely the verification of stroking time requirements, the calculation and analysis of the compressed air demand, and the overpressure protection of the whole network. The analysis showed that pneumatic stroking times are generally respected, however, 22 out of the 1012 valves require further design modifications since their safety functions are not, or are barely achievable with the current design. The consumption evaluation showed that the pre-determined criteria for maximum allowable flow rates is not respectable for more than 60 % of the investigated cases. On the other hand, the network's overpressure protection has been carefully designed by selecting a total of 168 Pressure Reducing Valves into the network.

Pneumatic stroke times are essential for opening and closing the TCWS's valves in both control and safety functions. ITER uses compressed air to operate these valves mainly due to the high static magnetic field in the vicinity of the Tokamak. This means the compressed air must flow through several ten meters of piping and tubing until it reaches the valve actuators from the compressor station. The accurate modelling of the layout is therefore important to calculate the forming mass flow rate between the two. The used software is AFT Arrow, a steady-state compressible flow modelling code verified for nuclear applications. The simulation uses the pressure declarations from the compressor side and the pressure required to open the valves from the available torque curves and actuator datasheets to determine its boundary conditions. Next, the hydraulic resistances are modelled by extracting data from the already available 3D model, and by writing a code base used to collect, organise, and declare resistance data, as well as to calculate the K-value for every AFT Arrow pipe entry. The network also includes valves, where the resistance data has been gathered from the manufacturers. To also consider the network effects reducing individual flow rates when multiple valves are operated simultaneously, scenarios are created in AFT Arrow. Once the models are ready, the software solves the relevant hydraulic equations and exports the forming mass flow rates per valve. This is then collected and organized by other VBA macros. The stroking times are then calculated using actuator, command, and valve function data. The study found that a total of 108 valves that do not comply with the stroke time requirements. 87 of them have no safety classification, and hence the thesis suggests sequential valve operation for these. The calculation also found that 21 valves with a Safety Function are not able to respect their stroking time requirements. This could compromise the plant's safety in case of a Loss of Coolant Accident, therefore significant design modifications are necessary. This may include spring-assist modifications or sizing a small pressure tank close to the location of these 21 valves. Lastly, a single valve with an associated safety function has been found to have an 18 % safety margin. Although this does not seem to be a possible issue, it takes away the possibility of stroke time control, and does not leave margin for considering degraded environmental conditions. To ensure reliability, the study suggests connecting the valve to a different compressed air interface point inside the same room, decreasing the number of safety-important valves connected to the same train.

Evaluating the compressed air consumption is important to determine whether the consumption can be supplied by the upstream compressor network or not. Due to ITER's unique layout, sizing the compressor is not the scope of the current assessment. Instead, the peak and continuous consumptions are calculated based on the pressurised actuator chamber volumes, the required pressure to open the valves, the required average stroking times, and operational considerations. The individual valve consumptions are then summed up per scenario and are declared for each interface point. The results indicate that several interface points are undersized, and for most, the pre-determined limit is likely to be exceeded during the system's operational lifetime. Five interface points show that the threshold is surpassed when a Safety Function is triggered, implying that additional measures will be necessary.

Protecting the network from overpressure is an equally important part of the sizing process. Several components of the 26CATC network are not able to tolerate the highest pressures declared by the upstream side. To protect the network yet still ensure valve opening under peak process loading conditions, the network is protected on the main line, and for some particularly vulnerable actuators, right before the actuators. To avoid locking the air in case of a fire scenario, bypass valves are included in parallel, as well as a Safety Relief Valve for each interface. The sizing process identified three suitable candidates for different sizing flow rates, and selected a total number of 168 Pressure Reducing Valves into the network.

Future work will focus on several high- and medium-priority actions aimed at improving system reliability and ensuring operational safety. The most urgent tasks include testing and analyzing the closing times of valves, as this has not been evaluated by this thesis. Additionally, the sizing of the pressure vessels to operate the safety-related valves on interface point 6511CA-VG-1285 takes priority. Furthermore, the engineering team needs to investigate efficient solutions for managing large interface point consumptions with the upstream engineers. Additionally, a detailed assessment will be carried out to determine how to safely operate non safety-important valves, defining the minimum operational pressure required at the interface—recommended at 8 barg—to ensure all valves function reliably under varying conditions. Medium-priority activities involve finalizing Arrow models and recalculating valve stroking times based on finalised 3D geometries, initiating Pressure Reducing Valve qualification and procurement while reassessing valve selection and sizing according to the newest consumption design results.

Bibliography

[1] A.G. Olabi and Mohammad Ali Abdelkareem. Renewable energy and climate change. *Renewable and Sustainable Energy Reviews*, 158:112111, 2022.

[2] Choyon Kumar Saha and Angela V. Carter. Phase-out or lock-in fossil fuels? least developed countries' burning dilemma. *The Extractive Industries and Society*, 11:101140, 2022.

[3] International Energy Agency. Global Energy System. `https://www.iea.org/world`, 2025. Last accessed: 10/03/2025.

[4] Govinda R. Timilsina. Are renewable energy technologies cost competitive for electricity generation? *Renewable Energy*, 180:658–672, 2021.

[5] Mihai Daniel Roman and Diana Mihaela Stanculescu. An Analysis of Countries' Bargaining Power Derived from the Natural Gas Transportation System Using a Cooperative Game Theory Model. *Energies*, 14(12), 2021.

[6] Mikalai Filonchyk, Michael P. Peterson, Lifeng Zhang, Volha Hurynovich, and Yi He. Greenhouse gases emissions and global climate change: Examining the influence of co2, ch4, and n2o. *Science of The Total Environment*, 935:173359, 2024.

[7] International Energy Agency. Energy Technology Perspective. `https://www.iea.org/reports/energy-technology-perspectives-2024`, 2024. Last accessed: 10/03/2025.

[8] ITER Organization. ITER Talks, 2018-2021. Accessible via ITER Intranet. Last accessed: 27 February 2025.

[9] ITER Organization. ITER website. `https://www.iter.org/`, 2025. Last accessed: 26 February 2025.

[10] D. Boilson X. Bonnin P. de Vries L. Giancarli Y. Gribov S.H. Kim M. Lehnen T. Luce I. Nunes A.R. Polevoi S.D. Pinches R.A. Pitts R. Reichle M. Schneider J. van der Laan G. Vayakis D.J. Campbell, A. Loarte. ITER Research Plan within the Staged Approach (Level III – Final Version). Technical report, 2024.

[11] ITER Organization. Far more than a fancy ashtray. `https://www.iter.org/node/20687/far-more-fancy-ashtray`, 2020. Last accessed: 10/03/2025.

[12] S. Ceropian. Defined requirement for ITER Cooling Water Systems (M369M3 v2.1). Technical report, ITER Organization, 2016.

[13] A. Bhatia. *Control Valve Basics: Sizing and Selection*. Last accessed: 12 February 2025.

[14] Emerson. *Control Valve Handbook*. Emerson, 6th edition, 2023. Last accessed: 28 February 2025.

[15] M. Bou. Safety Functions, Systems, Signals Definition for I&C CSS (3R7ECW v3.1). Technical report, ITER Organization, 2015.

[16] J. Elbez-Uzan. ITER Seismic Nuclear Safety Approach (2DRVPE v1.6). Technical report, ITER Organization, 2011.

[17] M. Giammei. Safety I&C specifications for TCWS (RW54RB v5.4). Technical report, ITER Organization, 2023.

[18] L. Afzali. TCWS Procurement Valve List v8.1. Technical report, ITER Organization, 2021.

[19] SART. SART Pneumatic Actuators' Catalogue. `https://www.sart-von-rohr.fr/produits/servomoteurs-pneumatiques/`, 2025. Last accessed: 07/02/2025.

[20] ITER Organization. Qualification report for accessories - Lot 1 and 3 Valves (7YYXU8 v2.0). Technical report, 2024.

[21] AIR TORQUE. AIR TORQUE Pneumatic Actuators' Catalogue. `http://rotech.fr/products/34/68/actionneurs_air_torque`, 2025. Last accessed: 07/02/2025.

[22] FLOWBUS. FLOWBUS Pneumatic Actuators' Catalogue. `https://www.flowbus.com/index/s3_documentation/images/EPR-Series%20Catalogue.pdf`, 2025. Last accessed: 07/02/2025.

[23] Chang Dae Park, Byung Ju Lim, and Kyung Yul Chung. Design verification methodology for a solenoid valve for industrial applications. *Russian Journal of Pacific Geology*, 9(1):677–686, 2015.

[24] L. Afzali M. Giammei. Strategy for Pneumatic Actuators, 2020.

[25] L. Afzali. Solenoids and AOVs for TCWS Pneumatic Actuators (24C2QD v3.1). Technical report, ITER Organization, 2021.

[26] AFT. AFT Arrow 9 Learning Centre. https://docs.aft.com/arrow/AFT_Arrow_Home_Page.html, 2025. Last accessed: 17/03/2025.

[27] M. Jiménez, E. Kurmyshev, and C. E. Castañeda. Experimental Study of Double-Acting Pneumatic Cylinder. *Experimental Techniques*, 44(3):355–367, 6 2020.

[28] N. Schiliuk. Piping & Instrumentation Diagram (PID) of 26CATC (8PD87A v3.0). Technical report, ITER Organization, 2025.

[29] Delgado Crespo E. IS-26-65-001 Interface between Liquid Gas Distribution (PBS 65) and Cooling Water System (PBS 26) v5.1. Technical report, ITER Organization, 2024.

[30] Various authors. Valve Load Calculation Reports. Technical report, ITER Organization, 2019-2025.

[31] ITER. Actuator & Accessory Datasheets ITER Tokamak Cooling Water System (6B4WPA v1.2). Technical report, 2021.

[32] F. Munoz. Final Design - PBS 62.11-14-74 and 63.61 - 04TSME - Specification for Design - Mechanical - Fluids Design - Buildings 11-14-61-74-External. Technical report, ITER Organization, 2017.

[33] M. Giammei. PBS26 TCWS CA Consumption (8ULVK6 v1.1). Technical report, ITER Organization, 2023.

[34] Aalberts Integrated Piping Systems. mastering pressure: the essential guide to pressure reducing valves. https://aalberts-ips.us/newsroom/the-essential-guide-to-pressure-reducing-valves/, 2024.

[35] Swagelok. Process Regulators. https://www.swagelok.com/downloads/webcatalogs/en/ms-02-492.pdf, 2025.

[36] Clippard. How Does a Quick Exhaust Valve Work? https://www.clippard.com/cms/wiki/how-does-quick-exhaust-valve-work, 2025. Last accessed: 17/03/2025.

[37] Energy Steel. Solenoid box drawing (7WVYTX Rev. 7), 2024.

[38] Energy Steel. Solenoid box drawing (AHRVN3 Rev. 2), 2024.

[39] Swagelok. Swagelok Hoses Brochure. https://www.scribd.com/document/652834033/Ms-01-180-Swagelok-Hoses-Brochure, 2025. Last accessed 19/02/2025.

[40] Crane CO. *Flow of fluids - through valves, fittings and pipe*. Crane Co., 1982.

[41] Michel A. Saad. *Compressible Fluid Flow*. Prentice Hall, 1985.

[42] Donald S. Miller. *Internal Flow Systems*. BHRA Fluid Engineering, 2nd edition, 1990.

[43] I.E. Idelchik. *Handbook of Hydraulic Resistance*. Begell House, 4th edition, 2007.

[44] International Society of Automation (ISA). Ansi/isa-75.01.01-2012 - flow equations for sizing control valves, 2012. Standard for control valve flow equations.

[45] Applied Flow Technology. AFT Arrow - Verification cases v9. https://docs.aft.com/arrowverification/AFT-Arrow9-Verification.pdf, 2023.

[46] M. Sorli, L. Gastaldi, E. Codina, and S. de las Heras. Dynamic analysis of pneumatic actuators. *Simulation Practice and Theory*, 7(5):589–602, 1999.

A

Additional pneumatic actuator control schemes

A.1. 3/2 Piloted Air Operated Valve for Fail Open/Fail Close Valves

This configuration employs a direct connection from the AOV, mounted on the actuator, to the CA line within the building. When the solenoid valve is energised, the compressed air activates Port 14 of the 3/2 AOV, enabling PBS65.CA to pressurise the internal chamber of the actuator. When the solenoid is de-energised or in the event of a failure, the springs push the air from the internal chamber to the atmosphere. This configuration ensures safe failure.

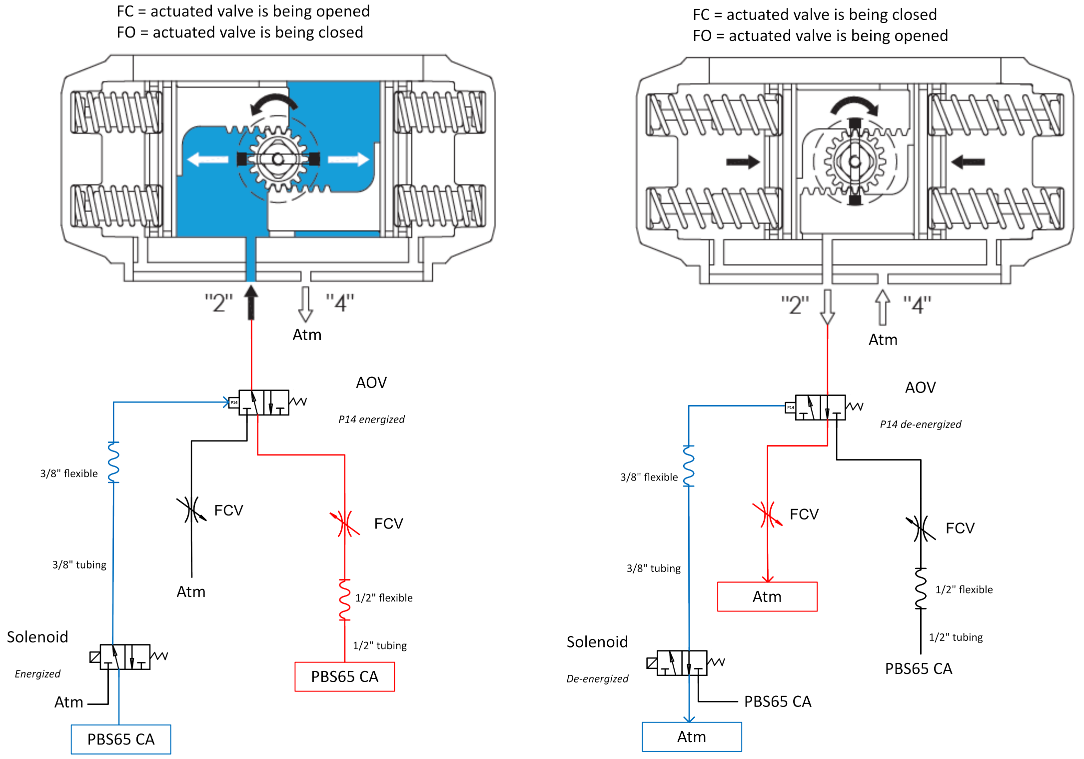

Figure A.1: Piloted AOV configuration for FO or FC valves. When the solenoid valve is energised (left), the pressure activates Port 14 of the 3/2 AOV, enabling PBS65.CA to pressurise the internal chamber of the actuator. When the solenoid is de-energised (right) or in the event of a failure, the springs push the air from the internal chamber to the atmosphere. Source: [25], modified by Marcell Szabo, 2025.

A.2. 5/3 Piloted Air Operated Valve for Fail in Position Valves

In this system, when the valve is opening, the left solenoid valve is energised. The compressed air then actuates the 5/3 AOV through Port 12, allowing PBS65.CA into the internal chamber of the FP double-acting actuator. This results in the expulsion of air through the same AOV to the atmosphere.

When closing the valve, the opposite solenoid is energised: it activates P14 of the AOV, positioning the valve to allow pressure to enter the external chamber. This then forces the air from the internal chamber to exit via the AOV.

When no solenoid is energised, the AOV remains in its last position. This ensures that CA is not connected to the actuator, preventing movement until a further command is received from the control system. In the event of failure or loss of CA on either the solenoid or AOV side, the valve stays in position, thereby achieving its fail-safe design.

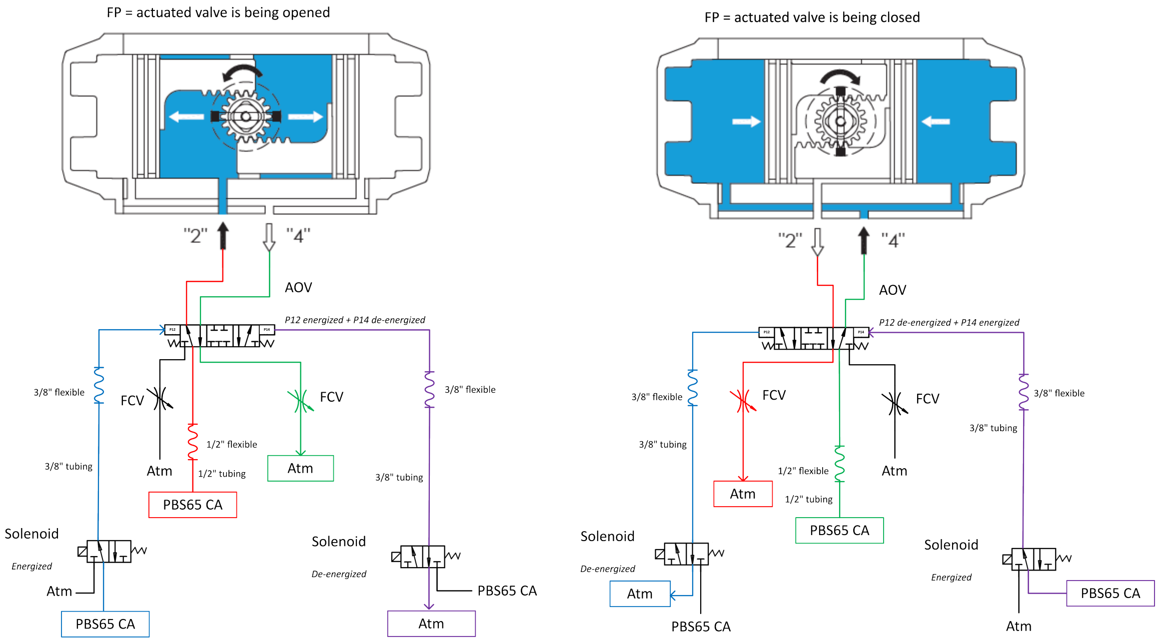

Figure A.2: Piloted AOV configuration for FP valves. When the left solenoid valve is energised, CA actuates the 5/3 AOV through Port 12, allowing PBS65.CA into the internal chamber, opening the valve. If the right solenoid is energised, it activates P14 of the AOV, allowing pressure to enter the external chamber. This then vents air through the AOV. Source: [25], modified by Marcell Szabo, 2025.

A.3. Air Operated Valves

As demonstrated previously, two separate AOVs are used in the system: a 3/2 for FC/FO valves and a 5/3 for FP valves. The first number denotes the number of ports, while the second indicates the number of routing configurations. A 3/2 valve has a single pilot port. When this port is energised, the pressure acts against a spring, causing the central rod to move into the position shown, allowing air to pass from Port 1 to Port 4. Conversely, when no pressure is applied to the pilot port, the spring pushes the central rod back, opening the path from Port 5 to Port 4.

5/3 valves are slightly different. These have two pilot ports, three inlets and two outlets. Air pressure is always applied on Port 1. When the left pilot is energized, air moves from 1 to 2 and from 4 to 5. When the right one is activated, air flows from 1 to 4 and comes back from 2 to 3. When no port is energized, the central rod stays in a middle position, blocking the air from every port, ensuring failure in position.

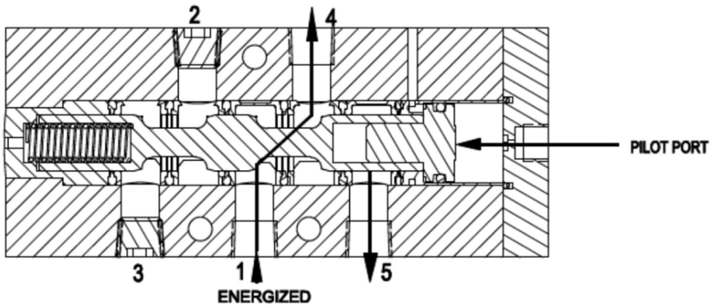

(a) 3/2 AOV. When the pilot port is energised, pressure acts against a spring, causing the central rod to move, allowing air to pass from Port 1 to Port 4. Conversely, when no pressure is applied to the pilot port, the spring pushes the central rod back, opening the path from Port 5 to Port 4.

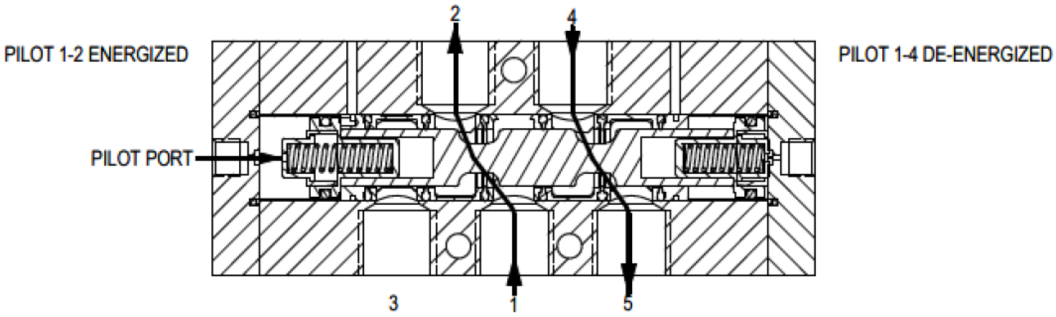

(b) 5/3 AOV. Air pressure is always applied on Port 1. When the left pilot is energized, air moves from 1 to 2 and from 4 to 5. When the right one is activated, air flows from 1 to 4 and comes back from 2 to 3. When no port is energized, the central rod stays in a middle position, blocking the air from every port, ensuring failure in position.

Figure A.3: Air Operated Valves (AOVs). Source: [31]

A.4. Flow Control Valve

Furthermore, to prevent water hammer effects within the TCWS, pneumatic control must account for the closing stroke time requirements. To enable adjustments and modifications to these closing times, Flow Control Valves (FCVs) are utilised. A flow control valve is a device that effectively throttles the flow through an adjustable stem. When longer stroke times are required, the stem is moved further into the flow, creating an increased pressure loss. This obstruction slows the flow, reducing the mass flow rate and thereby extending the stroke time.

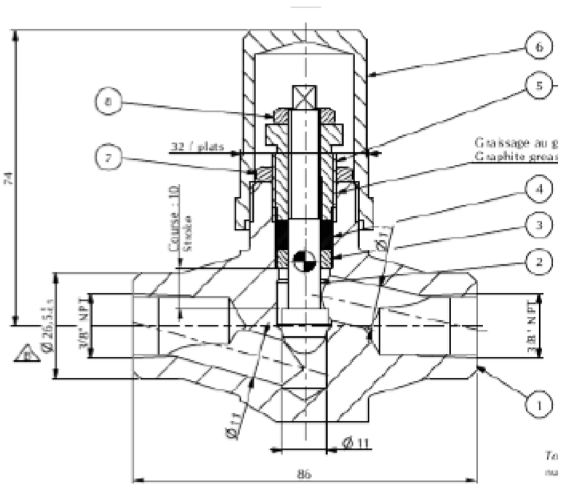

Figure A.4: Flow Control Valve. When longer stroke times are required, the stem (2) is moved further into the flow, creating an increased pressure loss and a throttling effect. Source: [31]

A.5. Quick Exhaust Valve

To avoid excessive stroke times in DC, a Quick Exhaust Valve (QEV) is incorporated. The depressurisation routing of pneumatic actuators proved too lengthy, necessitating a device capable of rapidly exhausting the remaining gas while maintaining routing integrity. The valve features a bat wing, which allows the fluid to pass into the actuator when pressurised from the inlet port. Upon pressure release, the bat wing closes the inlet port and vents the gas to the atmosphere.

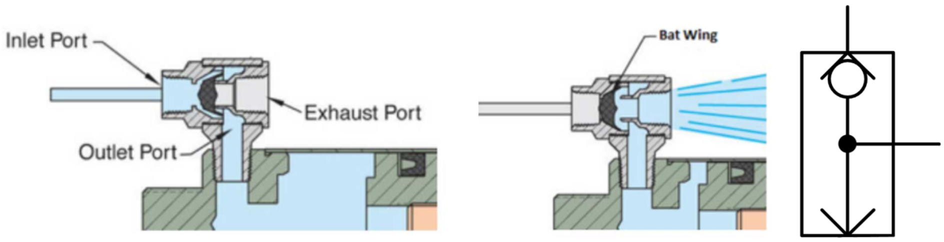

Figure A.5: Quick Exhaust Valve. The bat wing allows the fluid to pass into the actuator when pressurised from the inlet port. Upon pressure release, the bat wing closes the inlet port and vents the gas to the atmosphere. Source: [36]

A.6. Other compressed air network parts

Due to the high magnetic field within the Tokamak Building, it is necessary to implement magnetic shielding around the solenoid valves, increasing both their footprint and weight [24]. Additionally, a support box to house the associated solenoids is being developed for on-site installation. These solenoid boxes will be procured from Energy Steel or INOX [37] [38], and will determine the isometrics for the 26CATC routing.

The piping for the system was initially selected as DN25 network pipes and tubing, which will be modelled according to ITER requirements. The tubing roughness is assumed to be 1.5 µm (a typical value for stainless steel tubing, as opposed to 15 µm, which is typical for stainless steel piping). Flexible hoses [39], fittings, reducers, and expanders [31] are also components of the system and will need to be considered in the design.

B

Compressible Flow

B.1. Compressible Flow in 26CATC

The Stroke Time Verification Calculation uses compressible flow modelling to calculate the pneumatic stoking times of all 1012 actuated valves in TCWS. To determine the flow rates entering the valves, the calculation gives:

- the available pressure drop between the upstream interface point and the downstream actuators. This is given by boundary conditions on both ends of the network. These consider the minimum declared pressure upstream at the interface point, and a conservatively high pressure enough to actuate the TCWS valve.
- the hydraulic resistances of the piping network and the valve fittings along the compressed air routing.
- the likely operational scenarios when certain valves are actuated simultaneously. These include Safety Functions and system operation.

However, modelling the flow with these boundary conditions, resistances and scenarios remains the task of AFT Arrow. The present appendix hence aims to describe the compressible flow theory behind the flow rate solution of the code.

Compressible flow is a well-established phenomenon with extensive data available from various sources [40] [41] [42] [43]. As a fluid flows through instrumentation, it experiences losses from various sources, such as friction, changes in flow direction, and flow obstructions. For accurate pneumatic system modelling, understanding the flow behaviour and its resulting effects within the various network components is essential.

To start the analysis, one must identify the correct set of equations describing the specific problem. To do so, the network can be divided into two groups: pipes and fittings. The majority of the routing uses pipes to transport the air, while all other components can be treated as fittings - manufactured components used to connect, change the direction, or control the flow. Fittings can be elbows, bends, tees, wyes, but also control valves such as the Flow Control Valve or the Piloted Air Operated Valve. The next subsection presents the general governing equations for both categories.

B.2. Compressible Flow in Pipe

The two governing equations of flow are the continuity and momentum principles. Assuming 1-dimensional flow inside a straight pipe, the general equations simplify to:

$$\dot{m} = \rho A V = constant \tag{B.1}$$

where ρ is the density, A is the pipe area, V is the velocity, while $\dot{m}$ is the mass flow rate. The equation also states that, in a constant area pipe, any increase in gas density must be accompanied by a decrease in velocity.

The momentum principle for a constant-area straight pipe:

$$dP + f\frac{dx}{D}\frac{\rho V^2}{2} + \rho V dV + \rho g dz = 0 \tag{B.2}$$

where P is the pressure, f is the friction factor, dx and D are the pipe length and diameter, g is the gravitational constant, and dz is the change of height along the pipe section. Usually, the latter is negligible for gases.

B.3. Compressible flow through valves

To further investigate compressible flow in pneumatic networks, the flow through valves, branches and fittings is described in [40] [43]. These sources make it clear that no single uniform equation describes all possible fitting geometries. Therefore, to determine the corresponding hydraulic resistance of a fitting, the engineer can depend on the concepts of equivalent pipe length $\left(f\frac{L}{D}\right)$, resistance coefficient (K) or flow coefficient (C_V). Since the latter two are used at ITER, equivalent length is not described here.

The resistance coefficient K is derived from the Bernoulli equation and expresses the pressure drop across a component by linking it to the fluid's dynamic pressure. It is most commonly used for pipe fittings such as bends, elbows, area changes, and connectors.

$$K = \frac{\Delta p}{\rho\frac{v^2}{2}} \tag{B.3}$$

Although the Bernoulli equation does not strictly apply to compressible flow, most K-factor values in engineering handbooks are based on incompressible flow tests or theory [26]. As a result, even the careful application of handbook values carries some uncertainty. No universally accepted methods exist for determining K-factors in truly compressible flow, except in a few specific cases.

The flow coefficient (C_V) is defined by the ANSI/ISA-75.01.01-2012 standard [44] as the flow rate through a valve for a unit pressure drop at a given temperature. While primarily used for valves, an equivalent value can also be calculated for other fittings.

$$C_V = \frac{\dot{m}}{N_6 F_P Y \sqrt{X_{sizing} P_1 \rho_1}} \tag{B.4}$$

where $\dot{m}$ is the mass flow rate, while p_1 and ρ_1 are variables of state at the fitting inlet. N_6 is a numerical constant from the ANSI table, F_P is a piping geometry correction factor, while Y is the expansion factor accounting for the density change through the valve. X_{sizing} is the ratio of pressure loss across the valve compared to the inlet pressure. If the valve type and C_V are given, this can be calculated by iterating the mass flow rate across the network.

B.4. Compressible flow in Arrow applied to the 26CATC

The software starts by solving the fundamental continuity (Eq. B.1 and momentum equations (Eq. B.2) for every pipe element, as well as the pressure drop across the valves (B.4). Then it enforces the continuity equation at every given branch. For branch i, all connected pipes are iterated over, yielding:

$$\sum_{j=1}^{n_{pipes}} \dot{m}_{ij} = 0 \tag{B.5}$$

where $\dot{m}_{ij}$ denotes the mass flow rate in the pipe connecting junctions i and j. Similarly, applying the energy equation at branch i and summing over all connected pipes results in:

$$\sum_j \dot{m}_{ij} h_{ij} = 0 \tag{B.6}$$

or, equivalently, in terms of stagnation enthalpy:

$$\sum_j \dot{m}_{ij} h_{0,ij} = 0 \tag{B.7}$$

where $h_{0,ij}$ is the stagnation enthalpy at the junction–pipe interface.

Since the boundary conditions given are all pressure type, the code iterates on the mass flow rate and modifies the intermediate pressure values until a unique solution is found. Arrow employs a modified Newton–Raphson matrix method to achieve a system-level balance of mass and energy. A solution is achieved when the continuity (B.5) and energy equations (B.7) are satisfied at all branching points within the network. After convergence, Arrow performs a verification step in which it iterates through each junction, summing the inflows and outflows of mass and energy, and comparing these totals against predefined solution tolerances. If any junction is found to deviate beyond the acceptable limits, the software issues a corresponding warning in the output. Once the calculation converged, the software exports a single mass flow value for all downstream boundaries, i.e. the TCWS valve actuators. The study uses this flow value as the flow rate entering the actuator at any given moment after the pilot and solenoid delay.

B.4.1. Software Verification

In the 26CATC network, the main hydraulic resistances come from pipes and valves. Therefore, the verification of Arrow's calculations for flow results for both pipes and valves takes priority. The selected cases were 11 and 6, available in [45].

Case 11 - Flow of air through pipe, non-sonic

Case 11 [45] [41] solves a compressed air flow through a 50 m pipe with exit values of $T = 293$ K and $p = 150$ kPa, comparable to 26CATC. As stated in the exercise, only the exit boundary conditions are known. To define the problem in Arrow, the mass flow rate or the pressure must be known on both ends. Consequently, by calculating the mass flow rate from the outlet conditions and applying the continuity principle to the pipe, the inlet mass flow rate is defined, completing the modelling setup (Fig. B.1a).

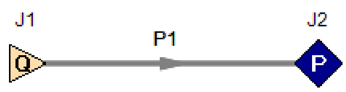

(a) Modelling setup in AFT Arrow

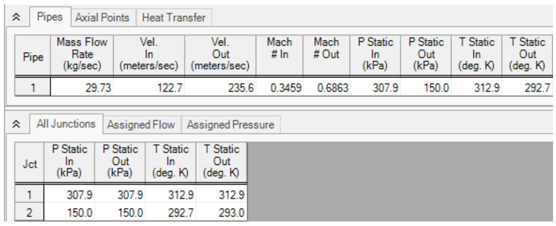

Pipes | Axial Points | Heat Transfer

Pipe	Mass Flow Rate (kg/sec)	Vel. In (meters/sec)	Vel. Out (meters/sec)	Mach # In	Mach # Out	P Static In (kPa)	P Static Out (kPa)	T Static In (deg. K)	T Static Out (deg. K)
1	29.73	122.7	235.6	0.3459	0.6863	307.9	150.0	312.9	292.7

All Junctions | Assigned Flow | Assigned Pressure

Jct	P Static In (kPa)	P Static Out (kPa)	T Static In (deg. K)	T Static Out (deg. K)
1	307.9	307.9	312.9	312.9
2	150.0	150.0	292.7	293.0

(b) Flow results from AFT Arrow

Parameter	Saad	AFT Arrow
M_2 – Mach number at exit	0.685	0.686
M_1 – Mach number at inlet	0.347	0.346
P_1– Static pressure at inlet (kPa)	306	308
T_1– Static temperature at inlet (deg. K)	312.76	312.9

(c) Results comparison between literature and Arrow. Source: [45]

Figure B.1: Case 11: compressed air flow through a 50 m pipe with given exit values [41].

As shown in Fig. B.1b & B.1c, the results of the literature and AFT Arrow agree on pipe flow.

Case 6 - Flow of steam through valve and bend, sonic

Case 6 was selected due to the flow being obstructed by a valve and a 90° bend. However, the fluid used in this example is steam, and the velocity is sonic. Still, this is the most similar example available in the literature to the 26CATC problems. The exercise describes a header feeding a digester with saturated steam through 30 feet of 2-inch piping, including a valve and a 90° bend. Both boundary conditions are pressure-type, 170 psia in the header and atmospheric pressure in the digester.

As demonstrated in the Verification Case, the Arrow results closely agree with the literature (Fig. B.2b), although some discussion was necessary. However, the verification model provided in the software package does not consider the K-factor of every specific resistance component separately, which gave room for testing with a modified model. By testing this way, a general conclusion can be deducted on the accuracy of built-in fitting libraries.

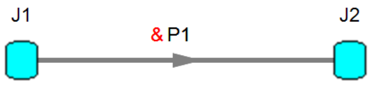

(a) Modelling setup in Arrow

Parameter	Crane Modified Darcy Formula	Crane Sonic Velocity Formula	AFT Arrow
Mass flow rate (lbm/hr) †	11,780	11,180	11,158
Exit Static Enthalpy (Btu/lbm)	N/A	1,196	1,149
Exit Temperature (deg F)	N/A	317	243

(b) Results comparison between literature and Arrow. Source: [45]

Figure B.2: Case 6 - sonic steam flow through a valve and a 90° bend. Exercise source: [40]

The modification was carried out by defining the fittings and losses in an extensive manner - such as the entrance from the header, a standard 90° bend, a standard globe valve, the exit to the digester, and the 30 feet, 2-inch schedule 40 pipe from a standard Arrow library. The loss definition is shown in Figure B.3, while the differences in flow results are organized in Table B.1.

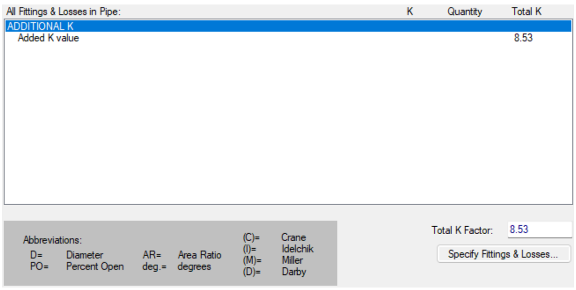

(a) Original definition of resistances in Arrow, with one K-factor.

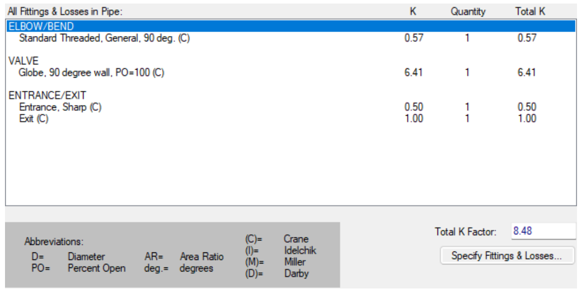

(b) Modified model with extensive loss definition.

Figure B.3: Modified setup comparison of Case 6.

Table B.1: Comparison between original (top row) and modified (bottom row) model

Mass Flow (lbm/hr)	Vel. Out (ft/sec)	Mach # Out	P Stag. In (psia)	P Stag. Out (psia)	P Static In (psia)	P Static Out (psia)
11158	1542.14	0.990	170	63.78	164.5	35.54
11176	1542	0.990	170	63.89	164.5	35.61

T Static In (°F)	T Static Out (°F)	fL/D + K	K	fL/D
363.4	243.0	11.86	8.53	3.33
363.4	243.1	11.81	8.48	3.33

Evaluation of flow results

It is clear from the table above that Arrow makes precise compressible flow modelling possible and has a very accurate built-in library of hydraulic resistances. It is important to mention that the limiting factor for preciseness in the design task is expected to be the complexity of isometrics, and the complexity in the dynamic behaviour of pneumatic actuators [46] [27].